



INSTITUT DE FRANCE  
Académie des sciences

# *Comptes Rendus*

---

## *Géoscience*

### *Sciences de la Planète*

Laurent Beccaletto and Sylvie Bourquin

**The Brécy depocenter as part of a new northern Massif Central  
Carboniferous–Permian Basin (France)**


Volume 355, Special Issue S2 (2023), p. 163-190

Online since: 18 December 2023

**Part of Special Issue:** Tribute to Jean Dercourt

**Guest editors:** François Baudin (Institut des Sciences de la Terre - Paris (ISTeP), Sorbonne Université), Éric Calais (École normale supérieure, Département de Géosciences, Paris) and François Chabaux (Institut Terre Environnement de Strasbourg (UMR 7063-Unistra-CNRS-ENGEES), Université de Strasbourg)

<https://doi.org/10.5802/crgeos.246>

 This article is licensed under the  
CREATIVE COMMONS ATTRIBUTION 4.0 INTERNATIONAL LICENSE.  
<http://creativecommons.org/licenses/by/4.0/>



*The Comptes Rendus. Géoscience — Sciences de la Planète are a member of the  
Mersenne Center for open scientific publishing*  
[www.centre-mersenne.org](http://www.centre-mersenne.org) — e-ISSN : 1778-7025



Research article

Tribute to Jean Dercourt

# The Brécy depocenter as part of a new northern Massif Central Carboniferous–Permian Basin (France)

Laurent Beccaletto <sup>Ⓜ,\*,a</sup> and Sylvie Bourquin <sup>Ⓜ,b</sup>

<sup>a</sup> BRGM, 45060 Orléans, France

<sup>b</sup> Univ Rennes, CNRS, Géosciences Rennes - UMR 6118, 35000 Rennes, France

*E-mails:* l.beccaletto@brgm.fr (L. Beccaletto), sylvie.bourquin@univ-rennes1.fr (S. Bourquin)

**Abstract.** The reinterpretation of deep wells and the reprocessing and interpretation of 115 km of industrial seismic lines can be used to update the geometry, depositional environments and tectonic evolution of the Carboniferous–Permian Brécy depocenter (southwest Paris Basin). The present-day geometry of the Brécy depocenter is controlled by several eastward dipping normal faults, some of which possibly connected to deep detachments that were active during the late Carboniferous–Permian history. It is estimated that the maximum thickness of the Brécy depocenter is 3900 m. The filling provides evidence for a thick late Carboniferous–lower Permian syn-rift stage overlain by a thin post-rift stage, probably similar to the tectonic evolution of the northeastward basins in the Lorraine region of France and Germany and thus attributed to the lower-middle Permian. The facies generally characterize lake environments, with occurrences of sediment supply attributed to fluvial, alluvial fan and delta fan deposits. They mainly display a retrogradational–progradational pattern during the syn-rift stage, and a retrogradational pattern during the post-rift stage. The Brécy area was part of a larger late Variscan basin during the latest Carboniferous–early Permian times in the northern Massif Central region.

**Keywords.** Late Carboniferous, Permian, Paris Basin, Deep well, Seismic interpretation, Regional correlation.

*Manuscript received 25 August 2023, revised and accepted 21 November 2023.*

## 1. Introduction

The late Carboniferous–Permian is a period of large-scale geodynamic reorganization, (i) with the final accretion of Pangea (Variscides/Mauretanicides/Alleghenides orogeneses) and the beginning of its breakup (NeoTethys opening) [e.g., Domeier and Torsvik, 2014, Scotese and Langford, 1995, Stampfli et al., 2013], coeval with (ii) the acme of the Late Paleozoic Ice Age (LPIA), constituting a turning point in

the climate regimes of the Paleozoic [e.g., Gastaldo et al., 1996, Montañez et al., 2007].

From the end of the Carboniferous onwards, the over-thickened and hot Variscan crust collapsed [late-orogenic collapse; Burg et al., 1994, Faure, 1995, Malavieille et al., 1990, Ménard and Molnar, 1988, Van Den Driessche and Brun, 1992], triggering the rise of high-grade metamorphic domes along low-angle detachment faults, and the development of half-graben or pull-apart multi-directional intramountain coal basins [Costa and Rey, 1995, Gardien et al., 2022, Malavieille, 1993, McCann et al.,

\* Corresponding author.

2008a,b, Ménard and Molnar, 1988, Van Den Driessche and Brun, 1989].

These late orogenic Carboniferous–Permian basins (hereafter LOCPB) therefore widely developed around 300 Ma in the internal parts of the belt south of the northern Variscan Front. They crop out in several limited locations in and around the Variscan basement of western Europe (Pyrenees, Massif Central, Brittany, Vosges–Black Forest, Alps, Harz), in close genetic relationships with major Variscan tectonic structures (e.g., Sillon Houiller, South-Hunsrück Fault; Figure 1 and related references).

They were filled with siliciclastic volcanoclastic continental material—from alluvial to lacustrine through fluvial environments—at intertropical latitudes [Donsimoni, 1990, Gand, 2003, Mercuzot et al., 2021, 2022, Schäfer, 2011, Schneider and Romer, 2010, Soreghan et al., 2020]. LOCPB were also accompanied by widespread intrusive and extrusive magmatic activity with a crustal or mantle origin with mostly felsic and rare mafic signatures [Neumann et al., 2004, Timmerman, 2004, McCann et al., 2006]. Apart from scientific research, LOCPB were extensively studied for their resources such as oil, gas, coal, uranium or other ore deposits [Bouchot et al., 1997, 2005, Courel et al., 1986, Delmas et al., 2002, Dill et al., 1991, Mascle, 1990], and more recently for geothermal [Aretz et al., 2016] or natural helium [Hauville et al., 2021] purposes.

In map view, they occur as small isolated and disconnected “basins” with incomplete sedimentary successions and numerous sedimentation and erosional gaps [e.g., Schneider et al., 2020]. Their present-day area does not reflect their initial extent and thickness, which can be explored by studying their subsurface prolongation beneath the Meso-Cenozoic sedimentary covers [Beccaletto et al., 2015, Mercuzot et al., 2021, Schneider and Scholze, 2018, Ziegler, 1990]. These basins usually reach thicknesses of several kilometers like, for instance, in the southern French Massif Central [e.g., Lodève, Carmaux—La Grésine; BRGM, 1989] or central Europe [e.g., Saar-Nahe and Thuringian Forest basins; Schneider and Romer, 2010]. Generally speaking, the ages of the LOCPB broadly range from Gzhelian to Guadalupian encompassing the Stephanian, Autunian, lower Rotliegend and part of the upper Rotliegend western European stages [ca. 303 Ma to ca. 270 Ma; e.g., Ducassou et al., 2019, Michel et al., 2015, Lützner

et al., 2020, Opluštil et al., 2016, Pellenard et al., 2017, Poujol et al., 2023, Voigt et al., 2022].

One recurrent question that arises from the study of the LOCPB is based on sedimentological, structural and temporal criteria: what are their regional correlations and extents? The answer to this question calls for the recognition of reference basins with enough useful data to make correlations. On one hand, recent advances in their age calibration using radiochronological methods have led to improved inter-basin comparisons [e.g., Ducassou et al., 2019, Mercuzot et al., 2023, Opluštil et al., 2016, Pellenard et al., 2017, Schneider et al., 2020, Voigt et al., 2022]. On the other hand, fewer significant works have been carried out recently on their structural pattern and tectonic evolution [Beccaletto et al., 2015, and references therein], and therefore the poor understanding of their tectonic framework limits their comparison at local or regional scales.

One good way to discuss the tectono-sedimentary history of hidden subsurface LOCPB is to use seismic data to look for them under their Meso-Cenozoic sedimentary cover given that they may be considered as fossil basins with preserved pre-Triassic depositional and structural patterns. We present new results from the interpretation of industrial seismic lines spanning 115 kilometers, while targeting the Brécyc depocenter in the southwest Paris Basin, which has recently been reprocessed within the framework of an International Continental Scientific Drilling Program proposal [ICDP Deepdust project; Soreghan et al., 2020]. First, we aim to discuss the structural features, thickness and tectonic evolution of the Brécyc depocenter and the related sedimentary filling using seismic and well data. Last, we compare and propose correlations between the Brécyc depocenter and other Carboniferous–Permian deposits in the northern Massif Central, as well as other places in France and Germany.

## 2. Geological setting of the Brécyc depocenter

The Brécyc depocenter is one of the three several-kilometer-thick depocenters recently revealed by the interpretation of reprocessed vintage seismic lines in the southwestern part of the Paris Basin [together with the Contres and Arpheuilles depocenters; Figures 1, 2; Beccaletto et al., 2015]. It has a roughly

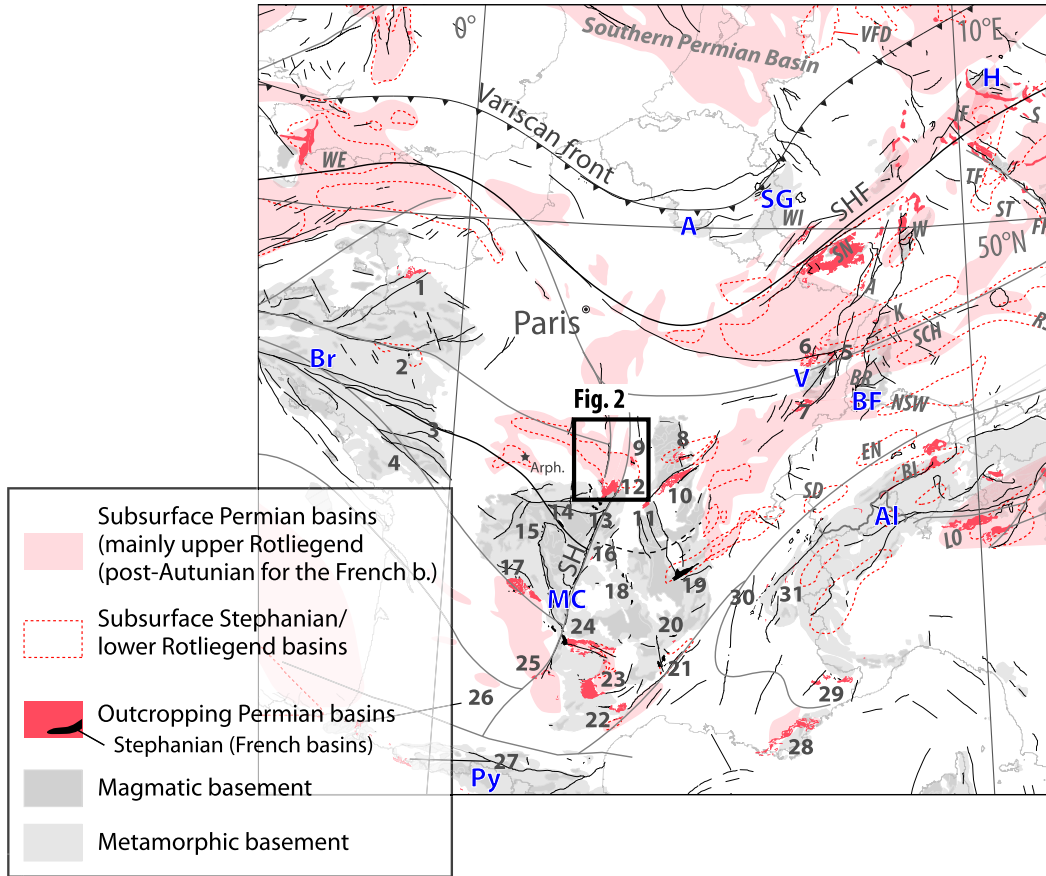


**Figure 1.** Map of NW European outcropping and subsurface LOCPB; compiled from Beccaletto et al. [2015], BRGM [1984, 1989, 2003], Delmas et al. [2002], Gast et al. [2010], Schäfer and Korsch [1998], Schneider and Romer [2010], Schneider and Scholze [2018]. *Numbers*—French outcropping LOCPB: 1: Carentan/Littry; 2: St-Pierre-la-Cour; 3: Doué-la-Fontaine; 4: Sillon Vendéen, Chantonnay, Faymoreau; 5: Villé; 6: St-Dié; 7: Ronchamp-Giromagny; 8: Autun; 9: Decize La Machine; 10: Blanzay-Le Creusot; 11: Bert; 12: Aumance; 13: Commentry, Doyet, Deneuille; 14: Ahun; 15: Bosmoreau-les-Mines; 16: Bassins du Sillon-Houiller; 17: Brive; 18: Brassac, Brioude; 19: St-Etienne; 20: Prades-Jaujac; 21: Alès; 22: Graissessac, Lodève; 23: St-Affrique; 24: Figeac, Decazeville, Rodez; 25: Quercy-Albigeois, La Grésigne; 26: La Rhune-Bidarray; 27: Ossau; 28: Var; 29: Barrot, Argentera; 30: Alpes zones externes; 31: Alpes zones internes. *Italic letters*—Other West European LOCPB A: Albersweiler; BI: Bifertengrätli; BR: Breisgau; EN: Entlebuch; FR: Frankenberg Bay (Naab—Weiden); IF: Ilfeld; K: Kraichgau (Baden-Baden); LO: Lombardian; MF: Manx-Furness; NSW: North Switzerland; S: Saale (Halle); SCH: Schramberg; SNB: Saar-Nahe; RS: Ries-Salzach; S: Sudetic; SD: Salvan-Dorenaz; ST: Stockheim; TF: Thuringian Forest; VFD: Variscan Foredeep; W: Wetterau; WE: Wessex; WI: Wittlich Graben. *Blue letters*—*Basement rocks* A: Ardennes; Al: Alps; BF: Black Forest; BM: Bohemian Massif; Br: Bretagne; H: Harz; MC: Massif Central; Py: Pyrenees; SG: Schieferer Gebirge; V: Vosges. Sillon Houiller fault: SH; South Hunsrück Fault: SHF. Arpheuilles-1 well: Arph.

elongated shape striking N30 parallel to the northern trend of the Sillon-Houiller fault zone. The opening of the basin was thought to be controlled by the activity of several N030-trending normal faults accommodating the deposition of the Stephanian-Permian deposits which have estimated thicknesses up to 3000 m.

The age of the Carboniferous–Permian series in the Brécy area comes from the description of the Bertray-1, Brécy-1 and Saint-Georges-sur-Moulon-1 well cuttings (from drilling reports; hereafter called the BTY1, BRC1 and SGS1 wells, respectively; Figure 2), and from palynological data from the core of the scientific Couy-1 well [Orszag-Sperber et al., 1992; hereafter COU1; Figure 2].

In the COU1 well, the sedimentary succession, attributed to the Permian based on the presence of several Darwinulacea ostracods [Orszag-Sperber et al., 1992], is composed of approximately 250 m of mainly red silty-clay sediments with sandstones and few conglomerates at the base. This succession describes a general trend from alluvial fan to shallow lake deposits; neither tonstein (volcanic ashes transformed into clay minerals) nor palynological data exist to shorten the age range [Juncal et al., 2018]. In this area, the Permian deposits end with the Triassic unconformity, overlain by middle Anisian deposits [Early and early-Middle Triassic gap; Bourquin et al., 2006, Juncal et al., 2018].

In BTY1, from 2963 m to 2842 m, the sedimentary succession is mainly composed of black-gray silty-clay interbedded with detrital coal, sandstones and conglomerates. The age is attributed to the late Carboniferous based on: gastropods and ostracods from the *Carbonita* genus found in the calcareous level at the base, bisaccate pollens at 2963 m and the presence of *Lycospora pellucida* and *Florinites junior* pollen at 2850 m [Bertray1, 1987].

In BRC1, below 1806 m, the facies are more carbonated with argillaceous-dolomitic limestones interbedded in fine-grained gray-green argillaceous sandstones. Between 1802 m and 1806 m, plant fragments suggesting a Carboniferous age [Brécy1, 1966] have been found in micaceous silty-claystone.

The drilling of the SGS1 well has reached a Paleozoic succession from 1639 to 1878.3 m attributed to the Cambro-Silurian by comparison with known facies in outcrops in the Massif Central [St. Georges-

sur-Moulon1, 1964].

In COU1, the basement, composed of metamorphic rocks, starts at a depth of 941.65 m. It is overlain by a highly tectonized Paleozoic sedimentary series [Lorenz et al., 1987] until 925.35 m. The Paleozoic upper part is composed of volcanoclastic deposits attributed to the Stephanian [Chantraine et al., 1992]; trachy-andesites sampled at the bottom of the Stephanian unit (925.35 m and 941.65 m) yielded an Ar–Ar plateau age of  $301.6 \pm 6.3$  Ma [Costa and Maluski, 1988]. The Stephanian volcanoclastic unit is overlain by Permian fluvio-lacustrine deposits above an angular unconformity [Lorenz et al., 1987].

### 3. Material and methods

#### 3.1. Seismic data reprocessing

The present study is based on the reprocessing of five seismic lines representing approximately 115 km, acquired by the ESSOREP oil company in 1984 and 1985 (CHER survey, denoted as CH; Figure 2). This new dataset completes the ca. 200 km of vintage industrial seismic reflection profiles that were reprocessed and interpreted in the Brécy area in the initial study of Beccaletto et al. [2015].

Given the acquisition parameters used in these exploration surveys, mainly the frequency bandwidth of the seismic source and the recording length (up to 4 s TWT—Two-Way-Time), the estimated depth of investigation is roughly 7–8 km, with a vertical resolution of approximately 25 m and 30–35 m respectively in the shallow and deepest part of the lines. These vintage seismic data have been reprocessed using modern Pre-Stack time migration (PSTM) methods and algorithms, thereby significantly improving the quality of the resulting seismic section and providing enhanced descriptions of the geological structures [Beccaletto et al., 2011, 2015]. Efforts were focused on three key steps that were repeated several times throughout the processing unit: (a) computing primary and residual static corrections in order to remove the topographic and velocity effects of the superficial rock layer, strongly affecting the seismic signal; (b) detailed velocity analysis; and (c) various methods of organized and random noise attenuation. Pre-stack time migration enhanced the details of the structural features and completed this reprocessing unit before stacking the data [cf. Laurent

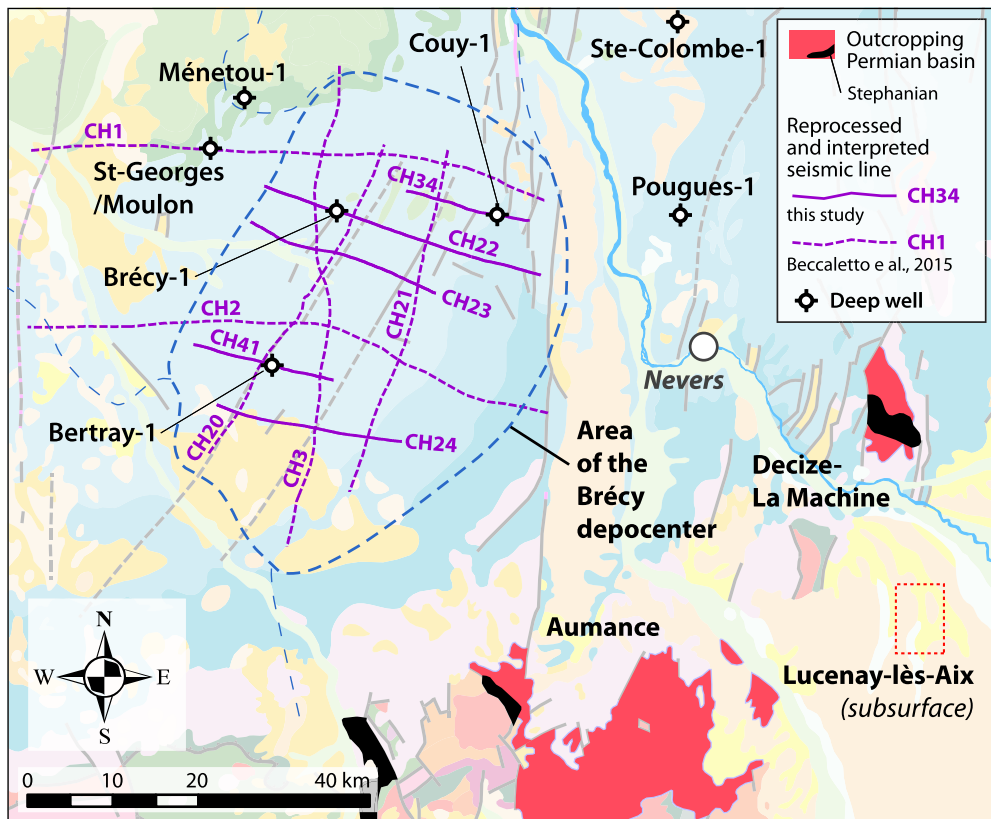


**Figure 2.** Geological map of the study area depicting the Brécly depocenter and adjacent LOCPB, the location of the reprocessed seismic lines, and deep wells. The geological background is from the 1:1,000,000 geological map of France [BRGM, 2003].

et al., 2021 for another example of seismic reprocessing and interpretation in Carboniferous basins].

### 3.2. Seismic interpretation and well-data

In a first step, the seismic facies and reflector geometries were interpreted by using nearby wells to calibrate and tie the seismic lines for the main horizons. Unlike the previous regional study of Beccaletto et al. [2015], the BTY1, BRC1 and COU1 wells are located directly on some of the newly reprocessed seismic lines (resp. CH41, CH22 and CH34; Figure 2), thereby preventing any lateral projection bias. Once the targeted horizons were identified near the BTY1 and BRC1 wells (deepest wells), they were correlated step by step, from line to line, by comparing the seismic facies using the Gverse Geophysics module of the Gverse suite (© Landmark), and by

checking their 3D structural consistency (using the 3D viewer of the interpretation software). Steps two and three correspond to the building of the structural scheme and the thickness map of the Brécly depocenter, respectively. In a fourth step, the electrofacies and depositional environments are described within the framework of the seismic interpretation by using subsurface well data such as: (i) the description of the cuttings from reports and well data (gamma Ray (GR), sonic or neutron, and resistivity) for the BRC1, BTY1, and SGS1 wells; and (ii) core description and complete well log data (GR, sonic, resistivity, density, photo electric factor (Pef), and neutron) for the COU1 well [Juncal et al., 2018]. In a last step, these four wells were correlated to give a lithostratigraphic and sequential framework to the Brécly area.

## 4. Results

### 4.1. Seismic interpretation, targeted horizons and seismic facies

Figures 3 and 4 display four examples of investigated seismic profiles in an uninterpreted and interpreted form. The main seismic features and units are discussed below from bottom to top.

The base of the late Carboniferous–Permian sedimentary fill (Base Basin Unconformity—BBU) corresponds to the top of the pre-Stephanian substratum. The four wells in the Brécý area do not reach the substratum, however it is cut across by fifteen wells in the westward Contres and Arpheuilles depocenters. There, the substratum could be sedimentary, metamorphic or plutonic [Beccaletto et al., 2015]. In most places, the top of the pre-Stephanian substratum matches the top of the acoustic basement, where the seismic signal becomes chaotic. However, some sets of reflectors, belonging to pre-Stephanian units, still appear locally below the BBU (line CH3, Figure 4).

The end-Carboniferous–Permian deposits s.s. correspond to the seismic facies observed between the Top Paleozoic Unit (TPU) and the BBU. In general, they are stratified with an overall wedge-shape geometry slightly thinning eastward, and continuous reflectors varying from low to high amplitudes and medium to high frequencies; chaotic or semi-transparent facies are also possible. The topmost preserved Permian beds display toplap geometries below the TPU (Figures 3 and 4). However, in closer detail, it is possible to distinguish three seismic sequences:

- (1) A *lower seismic sequence* with thicknesses less than 0.5 s TWT made of low-frequency/(very) high-amplitude, continuous to discontinuous reflectors; in the BTY1 well, these reflectors are correlated with Stephanian conglomeratic and coal beds, as seen in the Arpheuilles-1 well [Beccaletto et al., 2015];
- (2) a much thicker *intermediate seismic sequence* (up to 2 s TWT) with lateral thickness variations in units A, B and C; in particular, note the thickening of unit A toward the center of the basin. These three units were deposited during normal fault activity and, as a whole,

represent the syn-rift stage of the Brécý depocenter (cf. Section 5.1);

- (3) a thinner *upper seismic sequence*, (less than 0.25 s TWT), made up of unit D, located just below the TPU; this unit does not display any thickness variations related to fault activity. The seismic facies are more transparent here than in the lower and intermediate units, certainly due to less contrasting lithologies (cf. Section 4.1). The horizons of the *intermediate seismic sequence* display a toplap geometry beneath the base of the *upper seismic sequence*, indicating an erosional phase in between. This *upper seismic sequence* represents the post-rift stage of the Brécý depocenter (cf. Section 5.1).

The Mesozoic sedimentary cover of the Paris Basin unconformably overlies the Permian Brécý deposits and consists of parallel to sub-parallel continuous reflectors with medium- to high-frequencies and alternating medium- to high-amplitudes related to lithological variations within the Triassic and Jurassic deposits. The reflectors gently dip northward towards the center of the Paris Basin.

### 4.2. Fault patterns and structural schemes

All seismic lines display normal faults, which are the norm in the Brécý depocenter; the vast majority of the faults developed during the Meso-Cenozoic, as suggested by the equal down-throw all along the fault plane both across the Carboniferous–Permian and Mesozoic strata (blue arrows in Figures 3 and 4). Some faults characterized by different thicknesses of Carboniferous–Permian deposits on both sides are expected to have controlled the late Carboniferous–Permian filling. The seismic lines do not clearly image the prolongation of these normal faults through the base of the basin downward to the acoustic basement (Figures 3, 4). Deeply seated reflectors located in the prolongation of eastward dipping normal faults may correspond to low angle normal faults (detachments; Figures 3, 4; cf. Section 5.1). These initial Carboniferous–Permian faults also display Meso-Cenozoic activity, as shown by the down-throw of the TPU and overlying Mesozoic strata (black arrows in Figures 3, 4).

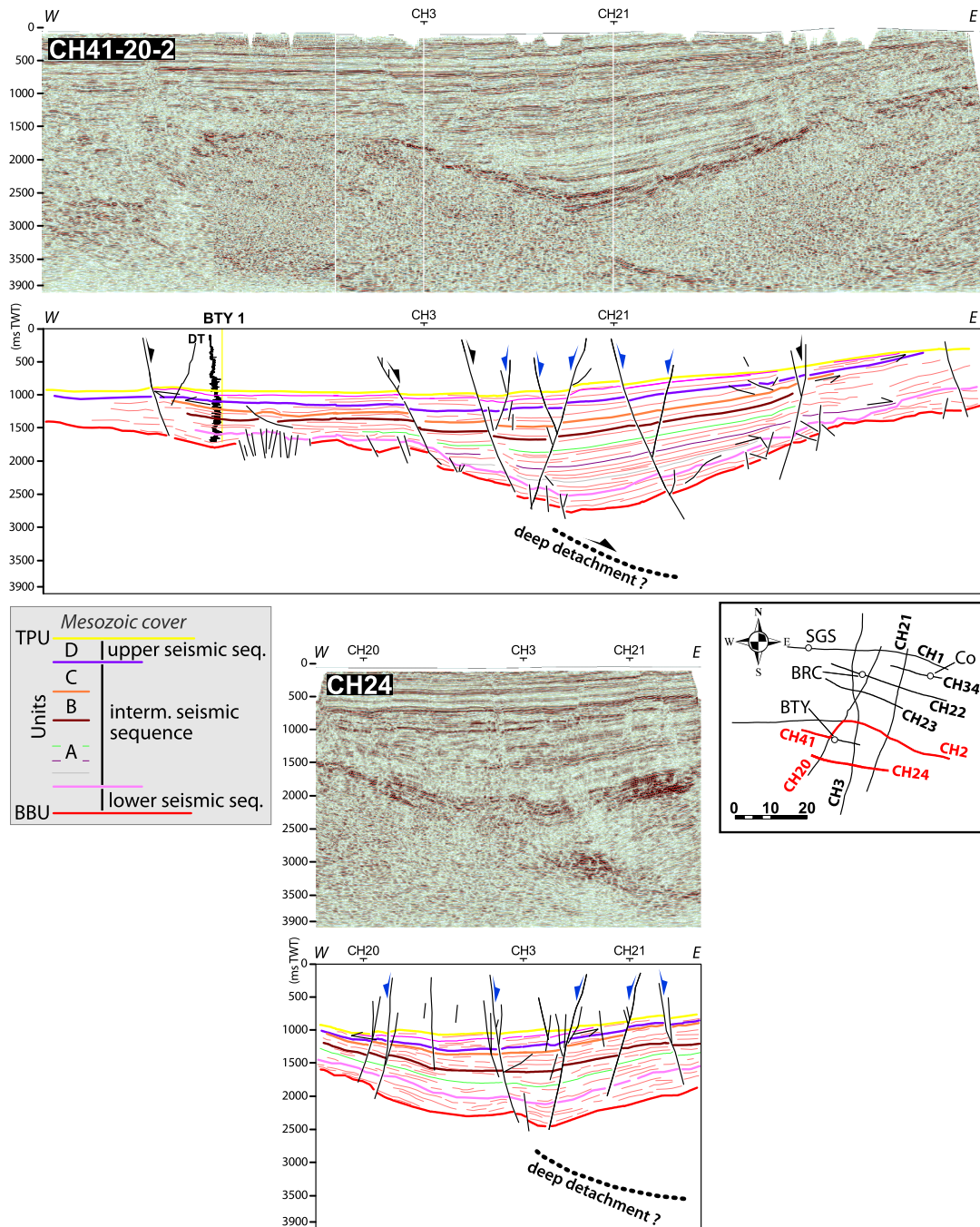


**Figure 3.** W-E composite line CH41-20-2 and line CH24, interpreted and uninterpreted, depicting the main structural features of the Brécý depocenter; blue arrows: Meso-Cenozoic faults, black arrows Carboniferous–Permian and Meso-Cenozoic faults; see text for details.



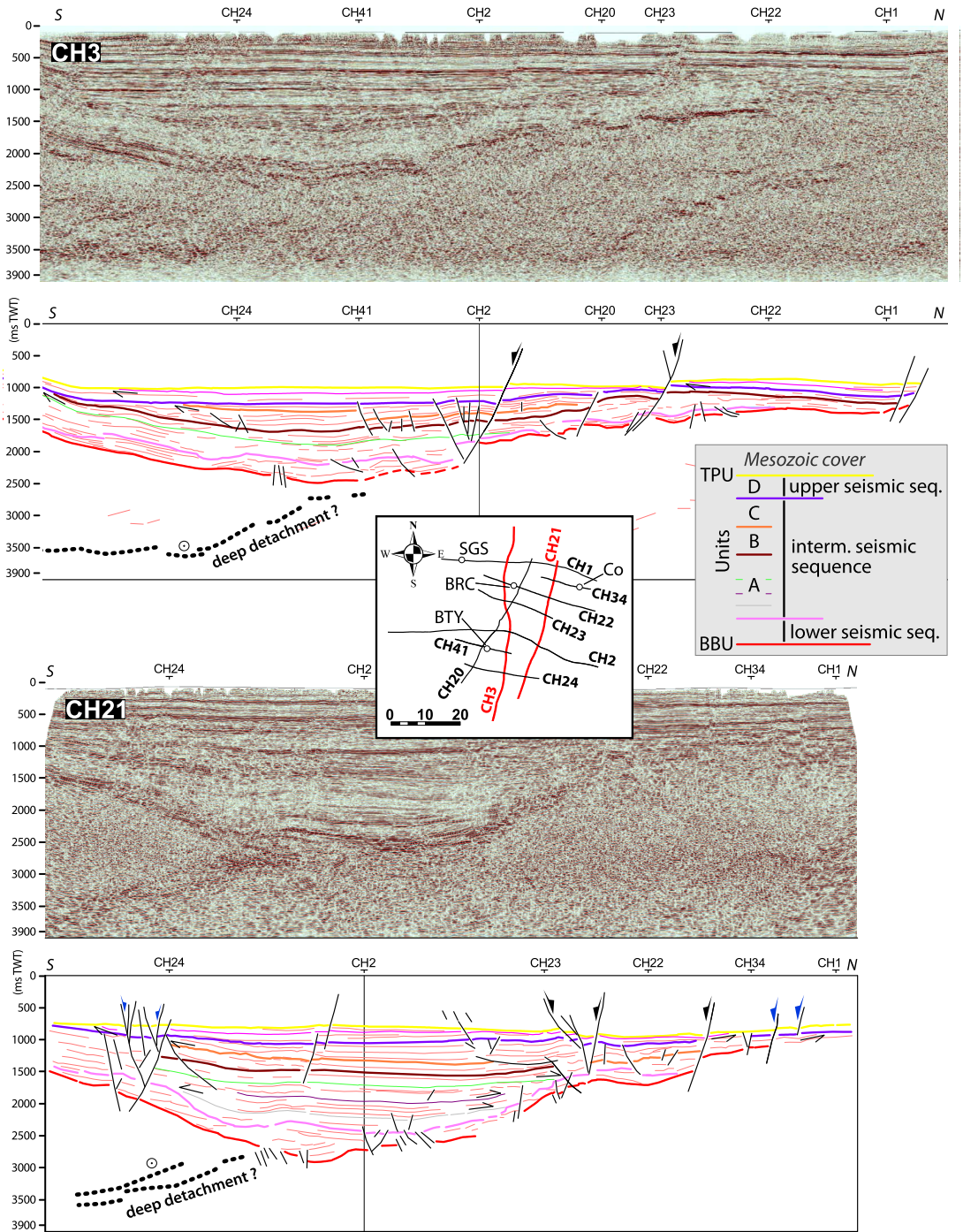


**Figure 4.** N-S line CH3 and line CH21, interpreted and uninterpreted, depicting the main structural features of the Brécy depocentre; blue arrows: Meso-Cenozoic faults, black arrows Carboniferous-Permian and Meso-Cenozoic faults; see text for details.

The reprocessing and interpretation of the additional seismic lines make it possible to build a detailed structural scheme for the Brécý depocenter, greatly improving the spatial resolution of the structural pattern drawn by Beccaletto et al. [2015]. The present study leads to the recognition of seven “major” faults (i.e., with a large cartographic extent and usually cutting through several seismic lines), and eleven secondary faults (i.e., cutting through one or two seismic lines to a lower extent; Figure 5). Most of these faults display an eastward dip, and only the antithetic fault has a westward dip. Their orientation varies between 20 and 40°N with an average value of approximately 30°N. As mentioned above, the structural pattern is actually a Meso-Cenozoic scheme, as all the faults—including those active during the Carboniferous–Permian—were active during the Mesozoic. We do not exclude the occurrence of smaller scale transverse faults (e.g., with N80 to N180 trends), but the numerous N30-trending faults may mask them and/or the density of the seismic dataset does not allow to discern them.

#### 4.3. Thickness maps of the Brécý depocenter

The new seismic dataset is used to accurately estimate the thickness of the Brécý depocenter (Figure 6). Thickness maps in TWT (then in meters) of the Brécý depocenter have been computed based on the interpreted horizons according to the following four steps methodology, by using the Gverse GeoAtlas module of the Gverse suite (© Landmark):

- Computation of grids in TWT for both the TPU and BBU horizons (these grids were calculated by interpolating the corresponding seismic horizons and faults).
- Computation of a thickness map in TWT of the Carboniferous–Permian sedimentary succession by subtracting the two previous grids.
- Calculation of an average interval velocity for the Carboniferous–Permian deposits from the BTY1, SGS1 and COU1 wells, all of which have identified Permian deposits. The velocity for each well is calculated from the thickness of the Permian in meters and in TWT from the seismic data, giving a value of 3778 m/s. We apply this “Permian” velocity to the whole filling, including (i) the intermediate

seismic sequence not fully reached by the three reference wells, because the seismic facies are similar suggesting similar lithologies, and (ii) the basal low-frequency/high-amplitude facies, because (a) they represent much lower thicknesses than the Permian deposits and are sometimes even missing, and (b) this velocity is very close to the one estimated in the Arpheuilles well [3615 m/s, Beccaletto et al., 2015; location in Figure 1].

- Computation of a thickness grid in meters by multiplying the thickness grid in TWT by the constant velocity of 3778 m/s.

As the thickness map is based only on the seismic data (there are no close outcropping geological contours to be used as hanging points), the map is hypothetical outside the zones where subsurface data are present. The resulting map displays the Brécý depocenter and its surroundings with an unprecedented resolution. The maximum thickness of the Carboniferous–Permian deposits reaches ca. 3900 m along the CH21 seismic line just south of the CH2 line; it is ca. 900 m thicker than originally expected [Beccaletto et al., 2015] due to a larger velocity value and better interpolation controls (because of the availability of more seismic lines). The minimum thicknesses—about 0 m—are located northeast of the main depocenter.

At the main depocenter, the maximum thicknesses of the *lower*, *intermediate* and *upper seismic sequences* are roughly 900 m, 2500 m, and 500 m respectively. The maximum thicknesses of the syn-rift deposits (*lower* and *intermediate seismic sequences*, A, B and C units) and post-rift deposits (*upper seismic sequence*, D unit) are ca. 3400 m and 500, respectively. In more detail, the maximum thicknesses of the A, B, C and D units are approximately 1600 m, 400 m, 500 m and 500 m, respectively.

The main depocenter has an elongated shape trending N60, which is slightly different to the average N30 trend of the scarce Carboniferous–Permian faults; in greater detail, it appears that the successive depocenters represented by the contour lines 3300 m, 3000 m, 2700 m and 2400 m display a clockwise rotation of their longest axis (inset in Figure 6). This could be the result of a dextral strike-slip component during the activity of the normal faults and the opening of the Brécý depocenter, either related or not to the activity of roughly W–E

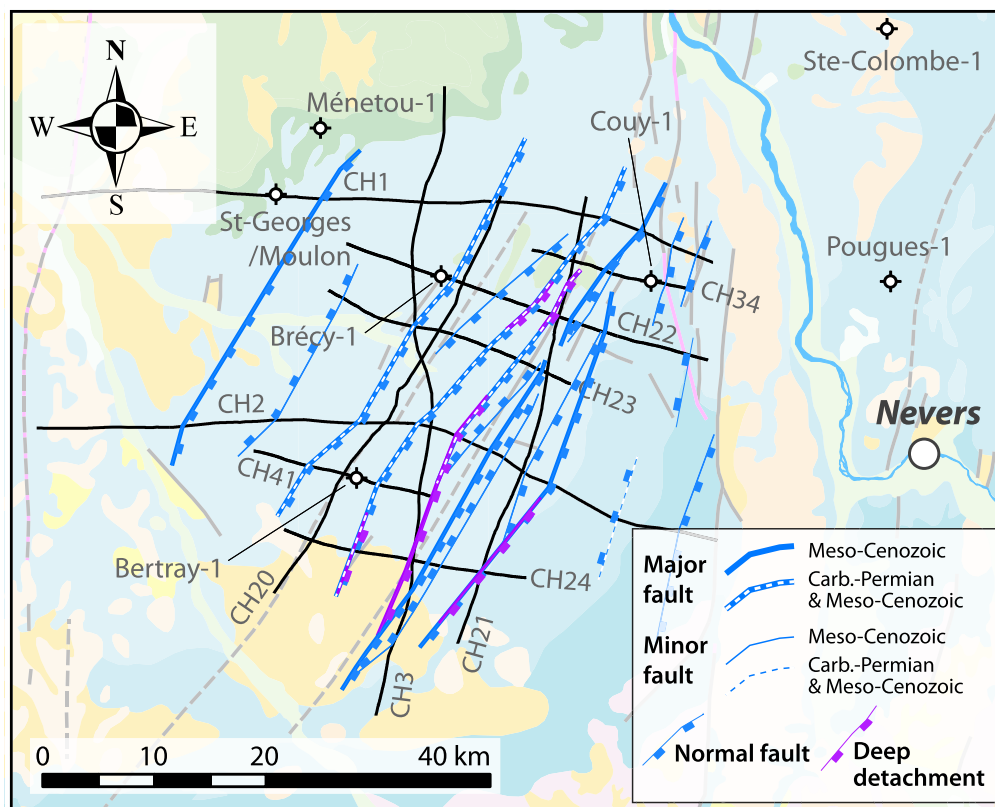


**Figure 5.** Structural scheme of the Brécy depocenter, depicting the major/minor faults, those with a Meso-Cenozoic tectonic activity or a Permo-Carboniferous and Meso-Cenozoic tectonic activity, and deep detachments; the geological background is from the 1:1,000,000 geological map of France [BRGM, 2003].

oriented normal faults (not depicted on the seismic lines as mentioned previously). Broadly speaking, the area displays a roughly SW-NE and then a W-E “thick” axis, located south of a roughly W-E oriented “thin” axis. These features suggest the combination of two deformational trends—N30 vs. W-E—the N30 trend is the only one expressed by normal faults. One hypothesis for this could be that the W-E trend is evidence of similar deeper trends that have already been identified in the basement [Baptiste et al., 2016].

#### 4.4. Depositional environment of the four reference wells

##### 4.4.1. Electrofacies description

The lithological evolution can be defined from each studied well using well-log data and the description of the cuttings.

Based on biostratigraphy data [Bertray1, 1987], the boundary between the Carboniferous and Permian is located at 2842 m. The lower Permian sedimentary succession is characterized by the Autunian facies [Bertray1, 1987], which is composed of, from base to top (Figure 7):

- from 2842 to 2260 m, by conglomerates (only until 2778 m) and coarse-grained sandstones characterized by low to medium GR (15 to 80 API) and Sonic (50 to 70  $\mu\text{s}/\text{ft}$ ) values, thereby evidencing low-porosity facies, alternating with clayey sandstones with GR from 80 to 120 API and Sonic below 60  $\mu\text{s}/\text{ft}$ , and brown silty-clay facies characterized by GR from 120 to 200 API and Sonic from 55 to 110  $\mu\text{s}/\text{ft}$ ;
- from 2260 to 1881 m, by brick-red micaceous silty-clay with traces of anhydrite and dolomite, (GR from 120 to 140 API and Sonic

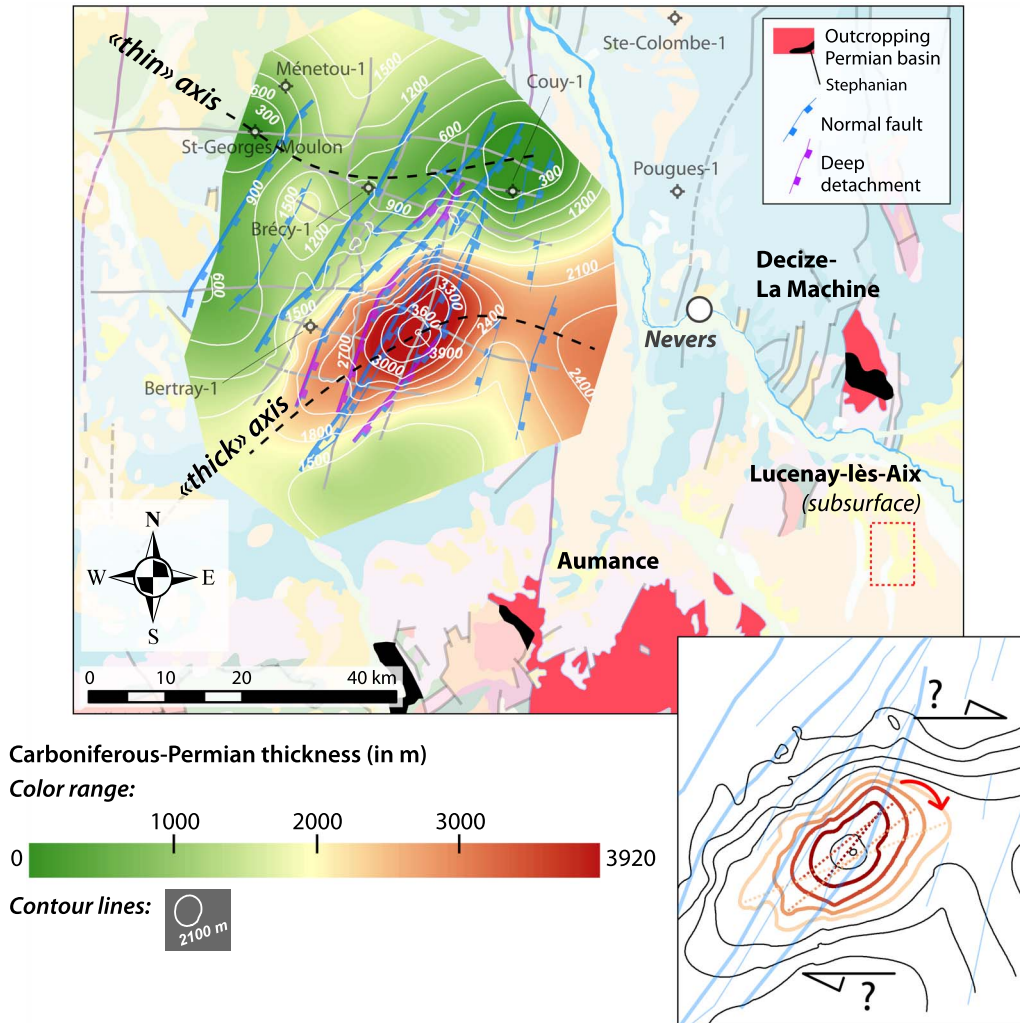


**Figure 6.** Thickness map (color range and contour lines) of the Brécly depocenter overlain by the structural map; the geological background is from the 1:1,000,000 geological map of France [BRGM, 2003]. Inset: clockwise rotation of the depocenters.

from 55 to 70  $\mu\text{s}/\text{ft}$ ), alternating with fine- to very fine-grained clayey micaceous sandstones (GR from 90 to 120 API and Sonic from 50 to 60  $\mu\text{s}/\text{ft}$ ), and white quartzite sandstones (GR from 45–90 API and Sonic from 40–50  $\mu\text{s}/\text{ft}$ ).

The upper part of the BTY1 well is composed of two distinct facies from base to top, the name of these formations is found in Bertrayl [1987]:

- the Upper Permian Sandstones Formation, from 1881 m to 1652 m, is characterized by

pink fine- to coarse-grained unconsolidated well-rounded sandstones (GR from 45–75 API and Sonic from 55–65  $\mu\text{s}/\text{ft}$ ), with few beds of conglomerates described from cuttings around 1800 m, and alternating with brick-red clay (GR from 90 to 130 API and Sonic from 75–90  $\mu\text{s}/\text{ft}$ ) or micaceous silty-clay (GR from 75 to 150 API and Sonic from 60 to 75  $\mu\text{s}/\text{ft}$ );

- the Upper Clay Formation, from 1652 to 1314 m, is composed of brick-red micaceous silty-clay with few beds of green clay in its upper

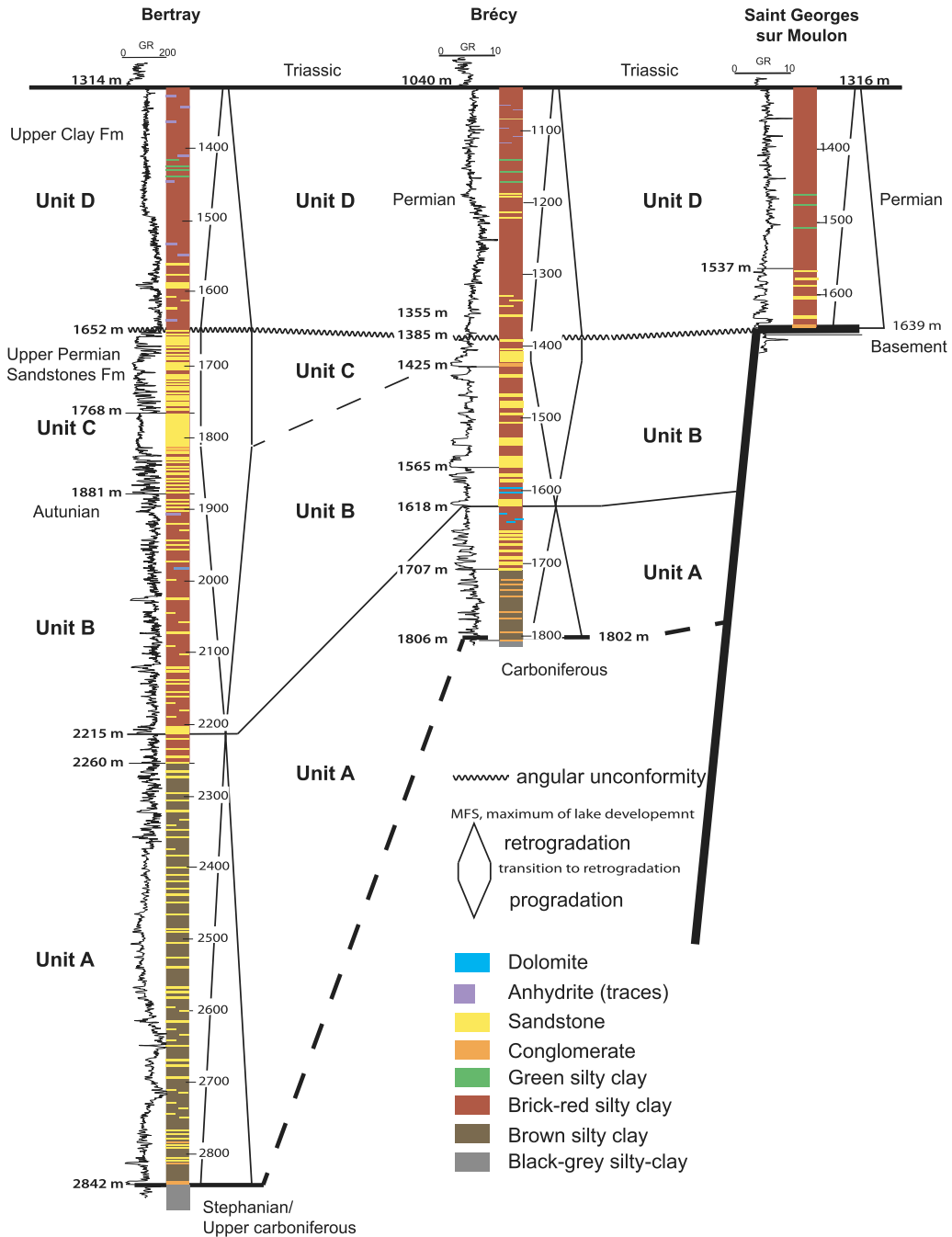


**Figure 7.** Correlations between the BTY1, BCY1 and SGS1 wells based on stratigraphic cycles.

part (GR from 90 to 150 API and Sonic from 40–80  $\mu\text{s}/\text{ft}$ ), and traces of anhydrite; this formation is sandier at the base.

The BRC1 well, drilled in [1966], is older than the BTY1 well [1987] and therefore has only GR in c/s, Neutron (c/s) and resistivity well-logs, and thus can

only be used to provide a qualitative comparison of the GR signal with the other wells (Figure 7). In Brécyl [1966], the Carboniferous is reached below 1802 m, and the sedimentary succession up to 1707 m has been considered as transitional facies from the Carboniferous to Permian based on conglomerates interbedded within brown-red micaceous silty-clay. Based on a previous seismic interpretation (cf. chapter 4.1) and well-log data, these facies are considered as Permian. Above 1707 m, BCY1 is considered as undifferentiated Permian Brécyl [1966] and has the following composition, from base to top:

- from 1707 m to 1565 m: coarse-grained sandstones to conglomerates interbedded with brown-red micaceous clay with carbonaceous clay around 1676 m, clayey sandstones and dolomitic nodules (highest resistivity and lower GR values between 1580 and 1651 m);
- from 1565 m to 1425 m, the sandstones, with sometime dolomitic cement, are interbedded in micaceous brick-red silty-clay;
- from 1425 m to 1355 m, the sandstones, interbedded with brick-red micaceous silty-clay, are pink, sometimes clayey, with a thin conglomeratic bed at the base of the sandstone level (lowest GR value and highest resistivity);
- from 1355 m to 1040 m, the succession is composed of brick-red micaceous silty-clay, sometimes green and interbedded with a rare and thin bed of fine-grained clayey sandstones (lowest GR value and highest resistivity) or traces of anhydrite and gypsum [Brécyl, 1966].

The SGS1, dated 1964, has only GR (c/s) and resistivity, and is considered as an undifferentiated Permian succession [St. Georges-sur-Moulon1, 1964] that is characterized from the base to top by (Figure 7):

- from 1639 m to 1537 m, conglomerates and fine- to medium-grained micaceous white to pink sandstones, sometimes dolomitic, interbedded with brick-red-brown micaceous and dolomitic silty-clay;
- from 1537 m to 1316 m, brick-red micaceous silty-clay with sometimes green

clay, rare sandstone levels and traces of anhydrite.

#### 4.4.2. Interpretation of depositional environment

An interpretation of the depositional environment evolution can be proposed by performing a comparison with adjacent areas. The wells with thicker and deeper deposits, i.e., BTY1 and BCY1, display different facies at the base of the succession with coarse-grained and conglomerate facies interbedded with brown silty clay facies, with scarce carbonaceous clays. These facies could attest to a sediment supply attributed to an alluvial fan or delta fan within deeper lake deposits as described southward in the Lucenay-lès-Aix area [Ducassou et al., 2019, Mercuzot et al., 2021].

Compared with the core description of COUY1 [Juncal et al., 2018], the mainly red silty-clay facies observed in the upper part of these wells (unit D, Figure 8), with some dolomitic beds, can be considered as a shallow lake. The sandstone and very few conglomerates, attesting to a sediment supply from a continental area, are attributed to an alluvial fan sediment supply within the lake [Juncal et al., 2018], the sediment supply is higher in COUY1 than in the three other wells (Figures 7, 8). This upper part of the sedimentary succession shows traces of anhydrite and gypsum from the description of the cuttings that could reflect an environment with more evaporation. However, given that only traces were observed and that no anhydrite has been observed in the shallow lake deposits of the COUY1 well [Juncal et al., 2018], we cannot exclude that these evaporites originate from the aforementioned Triassic deposits. Furthermore, the presence of paleosol developments may be indicated by dolomitic nodules and green clay facies, which could characterize either dolocretes or hydro-morphic paleosols [Retallack, 1988, Tabor and Montañez, 2004], such as those observed in the COUY1 well [Juncal et al., 2018].

The depositional environment of unit B (Figures 7, 8), compared with the lithology defined in units A and D, could be considered as fluvial or an alluvial fan in a lake environment, but with predominantly coarse-grained sediment from the continental area. The unconsolidated well-rounded pink sandstones described only at BTY1 (unit C) could be attributed to aeolian deposits, but due to the lack of core data, this is difficult to confirm.

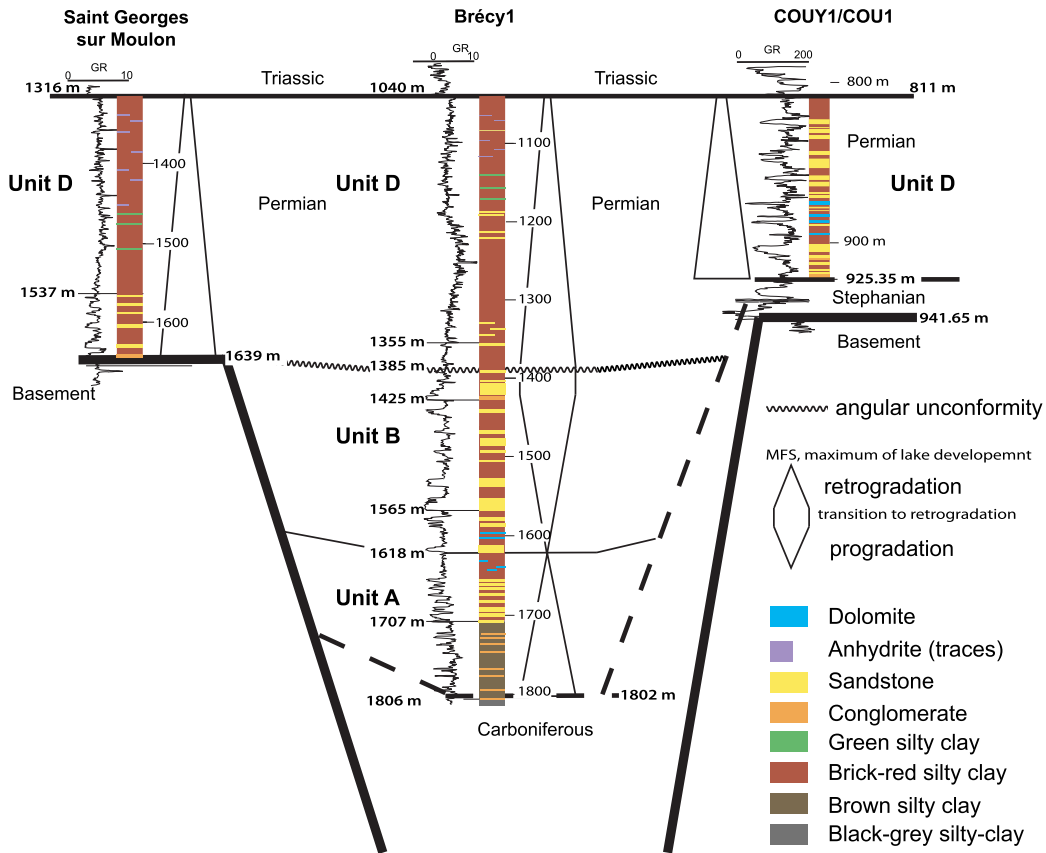


**Figure 8.** Correlations between the SGS1, BCY1 and COUY1 wells based on stratigraphic cycles.

#### 4.5. Sequence stratigraphy correlations

The correlations have been cross-checked with the seismic lines to maintain coherency between the well and seismic interpretations. We propose correlations between the four wells based on the electrofacies description and the vertical evolution of the depositional environment (Figures 7, 8). The most complete Permian sedimentary succession is observed in the BTY1 well. From 2842 m to around 2215 m, the vertical evolution from a predominance of conglomerates and sandstones to a predominance of silty-clay corresponds to unit A on the seismic lines (Figures 3, 4) and attests to a general trend towards an open lake (Figure 7). The sandstones and conglomerates can be attributed to alluvial or delta fan deposits in comparison with adjacent areas [e.g., Ducassou et al., 2019, Mercuzot et al., 2021, 2022]. After this maximum of lake development (Figure 7),

the clay facies become micaceous, sandier, and display some level dolomites indicating a shallower lake environment that corresponds to unit B on the seismic lines (Figures 3, 4). They vertically evolve to well-developed sandstone facies reached at 1652 m and correspond to unit C (Figure 7). This evolution from the maximum of lake deposits to the top of the sandstones attests to a general coarsening upward trend with more sediment supply around 1768 m (Figure 3). These sandstones are usually characterized by a clayey matrix and some conglomerate beds and could be attributed to fluvial or alluvial fan deposits; their upward evolution until 1652 m to unconsolidated well-rounded sandstones could suggest aeolian deposits interbedded within some red-silty clay facies. The general evolution, which corresponds to the *intermediate seismic sequence* (Figures 3, 4), allows to characterize a retrogradation and progradational trend from unit A to unit B

(Figure 7). Unit C may characterize the transition to a next retrogradational trend. However, it is difficult to define without core data, i.e., the sandstone recorded the transition from a progradational to retrogradational trend, and particularly if aeolian deposits are preserved [Bourquin et al., 2009, Olivier et al., 2023]. Moreover, based on seismic data, a well-defined angular unconformity has been defined at the top of unit C (i.e., in between the intermediate and upper seismic sequences; Figures 3, 4). As a result, unit D is not in continuity with the previous sedimentary succession. Above 1652 m, the sedimentary succession shows shallow lake deposits made of clay with some traces of evaporites, green clay and dolomitic nodules; the latter most probably represents some paleosol developments. This evolution characterizes a retrogradational trend (Figures 7, 8) ended by the Triassic unconformity and corresponds to the *upper seismic sequence* (Figures 3, 4).

For the BCY1 well, the whole sedimentary succession overlying probable Carboniferous deposits (top at 1802 m) is thinner than in the BTY1 well. A first trend is observed from conglomerates and sandstones until a maximum of lake deposits around 1618 m is reached (unit A; Figures 7, 8), correlated with the basal retrogradational trend of BTY1. A progradational trend, with well-developed sandstones and conglomerates evolving to fine-grained micaceous sandstones is observed until 1425 m (unit B; Figures 7, 8). Unit C is less developed in this borehole. Above the angular unconformity (1385 m), the same retrogradational trend as in BTY1 is observed, but with more sandstone and conglomerate deposits attesting to an area with more sediment supply (unit D; Figures 7, 8).

In the SGS1 and COU1 wells, the Permian sedimentary succession has a reduced thickness corresponding to a general retrogradational trend from conglomerates and sandstones to silty-clay facies. The latter corresponds to the same facies belonging to the upper retrogradational trend of the three other wells (unit D; Figures 7, 8), with the occurrence of more sandy beds in COU1 (Figure 8). In this well, eight retrogradational–progradational cycles were described based on core analyses within this retrogradational trend [Juncal et al., 2018], but in the absence of core data it is impossible to propose correlations at this high-resolution scale with the BTY1, BCY1 and SGS1 wells.

## 5. Discussion

### 5.1. *Tectonic evolution of the Brécý depocenter—regional comparisons*

The new seismic reprocessing greatly improves the understanding of the structural style of the Brécý depocenter, leading us to discuss the modality of its syn- and post-rift tectonic evolution (Figure 9), and to look for similar patterns in other LOCPB.

#### 5.1.1. *Syn-rift stage*

The new interpretation confirms and refines the multi-step widening scenario for the Brécý depocenter, controlled by the westward migration of a few successive active normal faults and their related depocenters, thinning and onlapping each other eastward (Figure 9). Some of the normal faults may be connected to deep detachments located in the pre-Stephanian basement, giving them a listric geometry at the time of the deposition (Figure 9). In fact, upper crustal extensional detachments in the footwall of LOCPB are a common structural feature around the Massif Central [Echtler and Malavieille, 1990, Burg et al., 1994, Faure, 1995, Gardien et al., 2022], and such detachments have been described close to the study area in the Autun and La Serre regions 150 km east of the Brécý depocenter [Choulet et al., 2012].

This induced the creation of an accommodation space that recorded a retrogradational trend characterized by well extended lacustrine deposits (unit A), followed by a progradational trend (unit B), due to increasing sediment supply in this subsiding context, before a probably new retrogradational trend (unit C) was abruptly ended by the angular unconformity (Figures 7, 8).

The intersecting N20-trending CH3 and CH21 lines are parallel to the main structural trend (Figure 6). There, the eastward facing normal faults are sub-parallel to the lines, so that they appear as flat lens-shape features subparallel to the BBU, disturbing the geometry of its reflectors. Deeply seated highly energetic reflectors in the basement below the BBU also occur and are similarly interpreted as potential extensional detachments planes.

All the above observations point to a syn-tectonic filling of the basin in an overall extensive tectonic regime during the latest Carboniferous–early



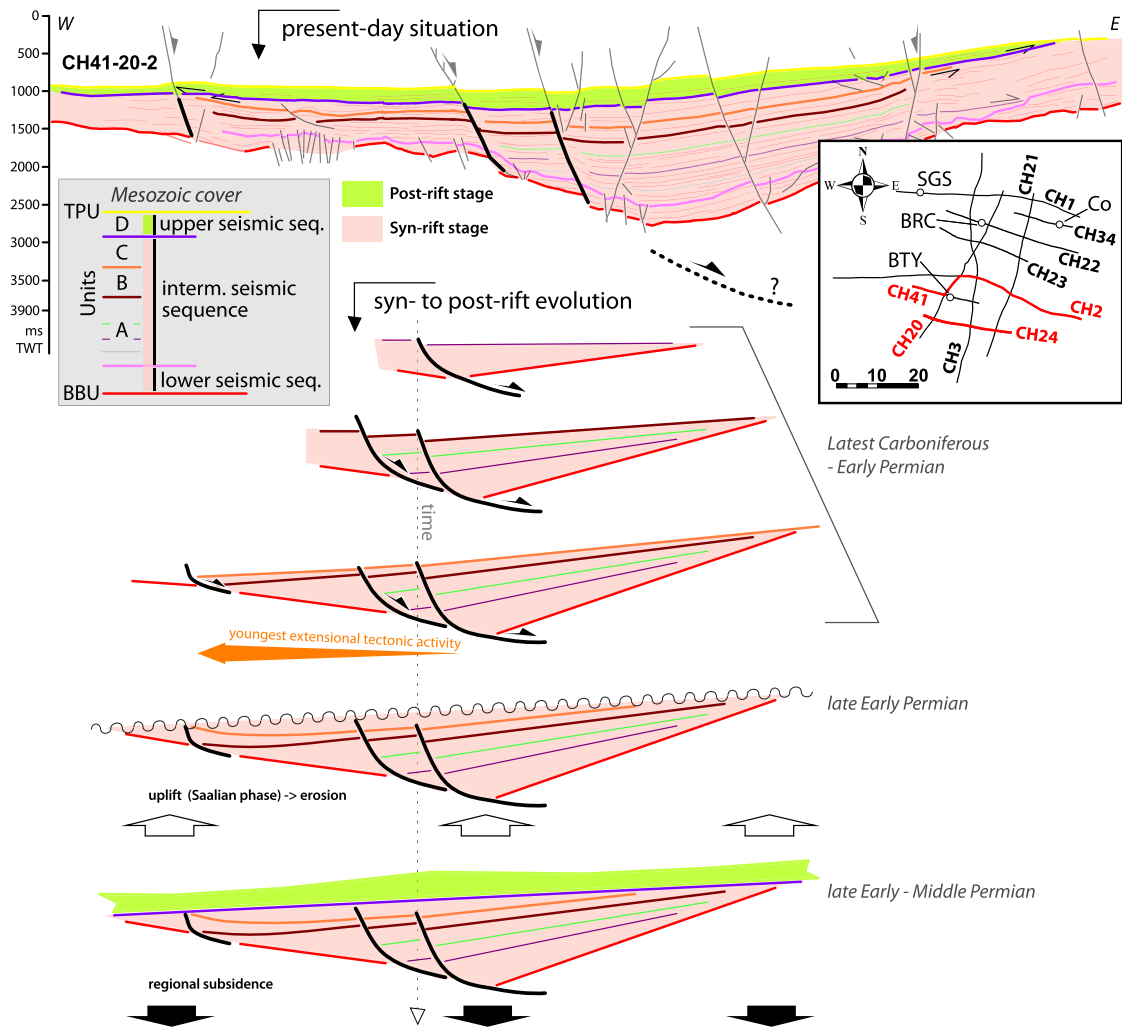


**Figure 9.** Present-day situation and tectonic evolution of the Brécý depocenter, using the representative composite CH41-20-2 seismic line. The syn-rift, uplift and post-rifts phases are successively depicted; the ages come from comparison with the Lorraine-Saar-Nahe Basin; see text for explanations.

Permian, characterizing the syn-rift stage of the Brécý depocenter. The maximum thickness of the syn-rift stage is ca. 3400 m.

5.1.2. *Post-rift stage*

The syn-rift activity is followed by a post-rift stage, whose occurrence is documented by the toplap geometry of the horizons of the syn-rift stage (mainly belonging to units B and C) below the first deposits of the overlying unit D (*upper seismic sequence*,

that corresponds to a new stratigraphic cycle where only its retrogradational phase is recorded due to an unconformity before Triassic sediment preservation) (Figures 5, 6, 9). The toplap geometries, observed in the whole area, provide evidence for the uplift and subsequent erosion of the syn-rift sediments before the deposition of the post-rift stage s.s. The latter is roughly isopach throughout the Brécý depocenter (ca. 0.25 s TWT, corresponding to ca. 500 m), and extends laterally beyond the

syn-rift stage. Another typical feature characterizing the post-rift stage is the absence of faults controlling the sedimentation. When considered together, these features suggest that the post-rift stage developed under a regional subsidence regime, which is certainly related to the late orogenic thermal relaxation of the hot Variscan crust [e.g., Averbuch and Piromallo, 2012, Vanderhaeghe et al., 2020, and references therein]. Toplaps of horizons belonging to the post-rift stage below the Triassic deposits suggest that the whole Brécý depocenter (i.e., syn-rift and post-rift stage) was then slightly tilted and subsequently eroded before the arrival of the first Triassic sediments. This erosional event may explain the relative low thickness of the post-rift stage (well depicted in the CH21, CH3 and CH41-20-2 seismic lines, Figures 5, 6). Beccaletto et al. [2015] checked and found similar geometrical and structural patterns in the adjacent Contres and Arpheuilles depocenters (thick syn-rift record beneath a thin isopach post-rift record).

The transition from a tectonic subsidence regime accommodated by discrete faults (syn-rift stage) to a regional subsidence regime (post-rift stage) through an uplift phase has not been documented yet in other French LOCPB, except in the Lorraine region (location in Figure 1). There, the latest Carboniferous–lower Permian syn-rift deposits are also controlled by listric normal faults rooting downward in deep decollement levels [Hemelsdaël et al., 2023]. They are then eroded following their uplift and tilting, before the arrival of the early to middle Permian post-rift sediments [Henk, 1993, Stollhofen, 1998]. The latter are then themselves eroded (toplap geometries below the Triassic deposits) before the deposition of the first Triassic sediments, as in the Brécý area [Hemelsdaël et al., 2023]. Further east in Germany, the Upper Rotliegend units of the Saar-Nahe (eastward prolongation of the Lorraine Basin), Thuringian Forest and Saale basins may also record these post-rift events [Hertle and Littke, 2000, Schäfer, 2011, Schneider and Romer, 2010]. In the literature, the tectonic phase responsible for the uplift is attributed to the end of early Permian Saalian phase [e.g., McCann et al., 2008a, Pharaoh et al., 2010, Stille, 1924, Ziegler, 1990], originally described in Central Germany, where folding and local tectonic inversion occur [Hertle and Littke, 2000, Kneuper, 1976]. In addition to the observations made in the Brécý depocen-

ter, the shortening phases recognized in some French LOCPB may also be related to this poorly known Saalian phase [Blès et al., 1989, Bonijoly and Castaing, 1983, Gélard et al., 1986, Genna and Debriette, 1994, Mattauer and Matte, 1998]. Going back to the Brécý area and according to this scenario, the base of the post-rift stage (unit D) would correspond to the superposition of two regional unconformities, i.e., the post-rift unconformity and the post-Saalian unconformity.

Lastly, it is unsurprising to not find explicit evidence of such a post-rift event in the French outcropping LOCPB, as the related deposits have certainly been partly removed by subsequent Meso-Cenozoic erosion [Barbarand et al., 2013, Guillocheau et al., 2000]. They are best fully described in subsurface settings beneath their Mesozoic cover, where the Permian deposits (including post-rift sediments) are still preserved and therefore accessible to seismic observations; in other words, the subsurface prolongation of other LOCPB around the Massif Central (e.g., Brive, Rodez, Saint-Affrique) may indeed preserve such post-rift deposits, even though they have not yet been identified. The recognition of a syn-rift stage followed by a regional uplift and a post-rift stage in the late Carboniferous–Permian Brécý depocenter is of great importance, as it allows to make a geodynamic connection with known LOCPB in eastern France and Germany. It confirms that the development of late Variscan basins is controlled by a large-scale (western Europe) underlying geodynamic event [e.g., the lithospheric delamination and removal of the Variscan mantle roots, e.g., Arnold et al., 2001, Averbuch and Piromallo, 2012]. Later, the arrival of the first Triassic sediments attests to the subsequent long-term Mesozoic thermal subsidence of the lithosphere, which led to the formation of the Paris Basin as a post-Variscan sag basin [Averbuch and Piromallo, 2012, Prijac et al., 2000, Robin et al., 2000].

### 5.2. *The Brécý depocenter was belonging to a much larger basin—local vs. regional correlations*

In addition to structural and tectonic aspects, which are difficult to understand without seismic data, another way to look for lateral correlations of the Brécý depocenter with neighboring basins is to track

the thicknesses of preserved end-Carboniferous–Permian deposits, their facies and paleoenvironments, and age similarities. In this section, we aim to connect the Brécý depocenter to the LOCPB of the northern Massif Central, before looking for wider-scale regional correlations.

First, as already demonstrated, the Brécý depocenter is undoubtedly connected westward to the Contres depocenter (which itself is connected to the Arpheuilles depocenter), as shown by the continuity of the Permian reflectors on the seismic lines between the three depositional areas [Beccaletto et al., 2015]. It is difficult to assess the occurrence of end-Carboniferous–Permian deposits north to northeast of the Brécý depocenter as there are no available seismic lines; this is also the case for its southwest prolongation. The few available spatially dispersed wells in these areas indicate that the Triassic deposits rest directly on basement rocks without intervening Carboniferous–Permian deposits (weathered granite in the Pougues-1 and Sainte-Colombes-1 wells, micaschists in the Ménétou-1 wells; location in Figure 2). It is however impossible to definitively conclude on the complete absence of Carboniferous–Permian rocks to the north of the Brécý depocenter based on such scarce data, as they may occur in between the wells. It could for instance be the case along the roughly N–S Loire-Sancerre fault zone and its northward prolongation as suggested by Delmas et al. [2002] (Figure 10). In addition, recent work done by the 45-8 Energy Company and BRGM leads to the recognition of new small subsurface Permian deposits southwest of the La Machine area [Hauville et al., 2021, Jacob et al., 2021]. This very local Permian occurrence may be connected to the Brécý depocenter, but their connection is not yet known.

Further south, it is strongly tempting to extend the Brécý depocenter to the outcropping Aumance Basin, although there is no direct evidence for this (no seismic line or well data). Extensive research has been carried out in the Aumance area for the purpose of uranium exploration, resulting in detailed sedimentological and structural descriptions based on numerous borehole and scarce seismic data [Mathis and Brulhet, 1990]. There, the Buxières Formation with gray Autunian facies has been dated close to the Carboniferous–Permian transition [ $298.59 \pm 0.35$  Ma, CA-ID-TIMS method, Mercuzot

et al., 2023; Figure 11]. This formation is overlain by red Autunian alluvial to lacustrine facies (Renière Fm.). Both facies are similar to those belonging to the intermediate seismic sequences (units A and B) of the Brécý depocenter. When considered together, these facies provide evidence for a syn-rift stage [Mathis and Brulhet, 1990, Paquette, 1980]. Note that the Aumance is not located along strike of the N30-trending Brécý depocenter, but instead is shifted to the east, such that the former should not be seen as the southward prolongation of the latter but as a parallel basin (Figure 10).

Eastward, recent works from Mercuzot et al. [2021, 2022] suggest the connection of the Decize-La-Machine (including the Lucenay-lès-Aix depocenter), Aumance, Autun and Blanzý-Le Creusot Stephano-Autunian basins: their lacustrine environments (from alluvial fan/fan delta to deep lake) and depositional ages are similar [latest Carboniferous to early Permian; Ducassou et al., 2019, Pellenard et al., 2017]. Here again, the Permian facies are similar to the intermediate (units A) seismic sequences of the Brécý depocenter, and they display seven retrogradational–progradational cycles within a general retrogradational trend ended by an unconformity overlain by Triassic deposits [Mercuzot et al., 2021]. Even though we observed the same general retrogradational evolution in the Brécý area (unit A), it is not possible to make a detailed comparison between these two areas because no age is available at the top of the Permian in the Decize-La-Machine area. Consequently, the absence of sandstones in units B and C (i.e., mainly a progradational trend) in Decize-La-Machine is either due to the erosion of these units or to a local sediment supply in the Brécý area, which is not recorded in Decize-La-Machine. However, a significant difference lies in the cumulative thickness of the deposits, which are unsurprisingly much lower in the outcropping basins (ca. 1 to 1.2 km) compared to the Brécý depocenter (2.5 km; Figure 11). Such large cumulative thicknesses are only reported from the Blanzý-Le Creusot composite basin, where more than two kilometers of Stephano-Autunian deposits are described from coal exploration boreholes [Figure 11, BRGM, 1989, Gand, 2003]. Further east, structural connections between the Autun, La Serre, Burgundy and southern Vosges basins have also been proposed [Choulet et al., 2012].

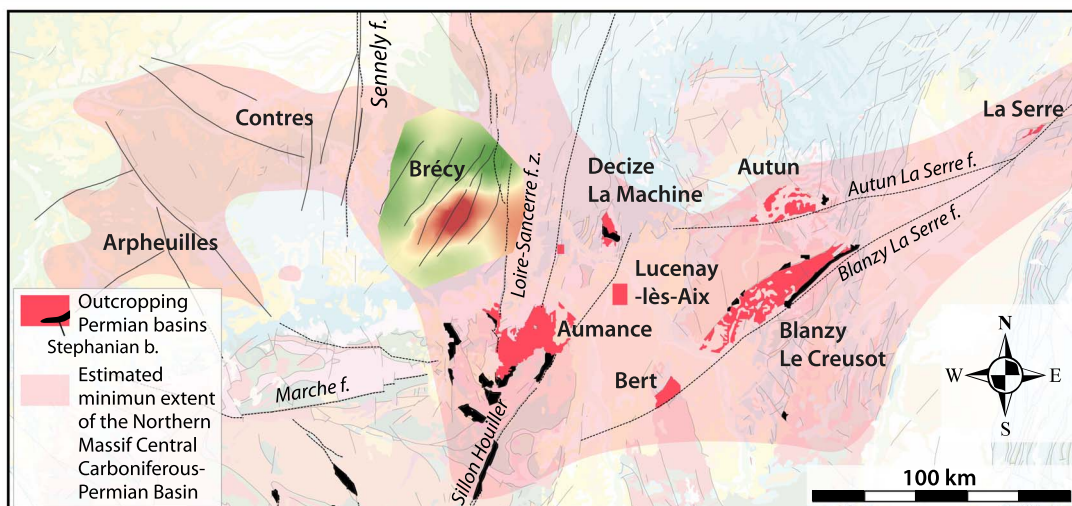


**Figure 10.** Estimated extent of the “northern Massif Central Carboniferous–Permian Basin” on a present-day geological map; the geological background is from the 1:1,000,000 geological map of France [BRGM, 2003].

All these observations and interpretations, correlating neighboring basins to each other, imply that these present-day isolated outcropping and subsurface basins, represented by the Stephano-Autunian facies, were part of a larger basin during the latest Carboniferous–early Permian. This larger basin encompassed the subsurface Arpheuilles, Contres and Brécly depocenters and the eastward smaller outcropping basins, spanning more than four hundred kilometers in length, with a roughly W–E trend (“northern Massif Central Carboniferous–Permian Basin”, Figure 10). These regional connections are also confirmed by paleobiogeography data from freshwater shark remains found in the Stephano-Autunian sediments, suggesting connections between all the French LOCPB of the northern Massif Central [including the Aumance, Autun and Blanzly-Le Creusot basins as well as on a much larger scale as far away as Germany; Luccisano et al., 2021, Fischer et al., 2013, Schneider et al., 2020].

It is important to note that the area depicted in Figure 10 (pale blue color) may represent a *minimum* extent of this wide basin. Indeed, some upper Carboniferous and lower Permian deposits have certainly been removed through time and are therefore lacking, due to (i) the erosion phases known before the arrival of the Triassic sediments [as discussed above and in Beccaletto et al., 2015], and

(ii) the Meso-Cenozoic uplift of the Massif Central area and subsequent erosion [Barbarand et al., 2013, Guillocheau et al., 2000].

On a wider scale, unlike the northern Massif Central, several-km-thick Stephano-Autunian deposits are encountered in several LOCPB of the southern Massif Central. These basins, such as Brive, Decazeville-Rodez, Carmaux-La Grésine, Saint-Affrique or Graissessac-Lodève, display similar Stephano-Autunian facies and ages to those observed in the Brécly depocenter and connected smaller basins, and reach thicknesses of up to four kilometers [Figure 11; BRGM, 1989, Pochat and Van Den Driessche, 2011, Poujol et al., 2023]. Due to the lack of subsurface seismic data, their extensional structural control is rarely imaged [Serrano et al., 2006 for a counterexample in the Aquitaine Basin] and is inferred from indirect observations [Chen et al., 2006, Pochat and Van Den Driessche, 2011].

Such thick series are also known in the LOCPB of Germany, for example in the Saar-Nahe and Thuringian Forest basins [Schneider and Romer, 2010, Schneider et al., 2020]. There, studies benefit both from favorable outcrop conditions and a large range of subsurface dataset including seismic lines. Consequently, the sedimentary facies and paleoenvironments are well constrained, the lithostratigraphic and extensional structural features are

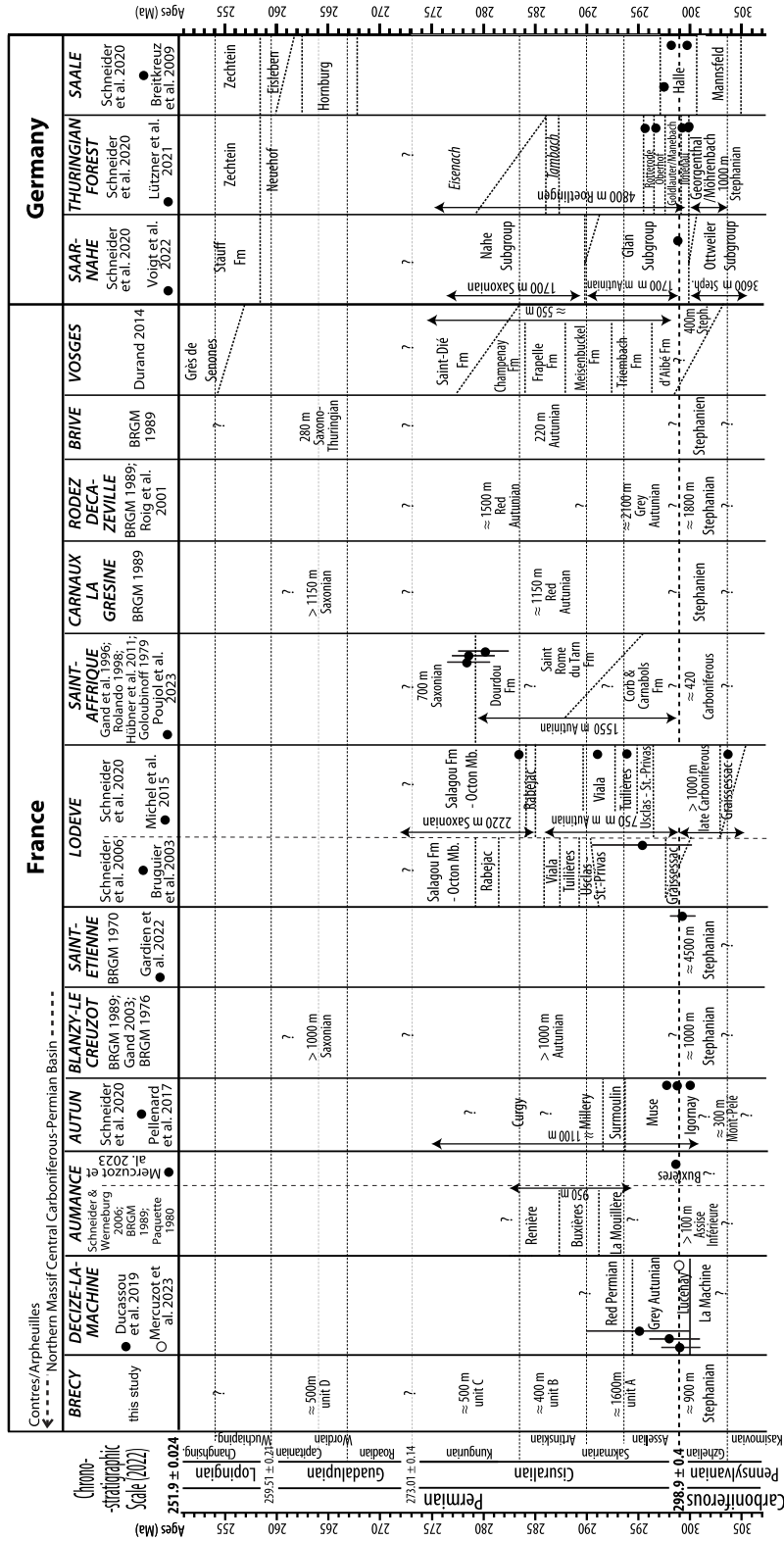


Figure 11. Compilation of thicknesses and ages of the main LOCPB in France and Germany, including the Brécy depocenter as a part of the “northern Massif Central Carboniferous–Permian Basin”.

well described, and recent absolute depositional ages are available [Henk, 1993, Stollhofen, 1998, Schäfer, 2011, Lützner et al., 2020, Voigt et al., 2022; Figure 11]. Based on all of these characteristics, they can be considered as other robust reference basins for large-scale LOCPB correlations.

All other LOCPB occurrences in western Europe generally occur in deformed areas as small, isolated patches with low preserved thicknesses, like in the Pyrenees (French and Spanish sides), Cantabria, Sardinia and the Alps and surrounding areas (France, Italy, Switzerland) [Barnolas and Chiron, 1996, BRGM, 1989, Capuzzo et al., 2003, Cassinis et al., 2012, Knight and Álvarez-Vázquez, 2021, Lloret et al., 2018, Pittau et al., 2002, Toutin, 1980]. We should also mention the supposedly wider basins with uncertain boundaries, thickness and age attributions that are also known offshore based on seismic data [e.g., Bay of Biscay, Western Approaches; Bois et al., 1991, Ziegler, 1990]. These characteristics make all these basins unsuitable for reliable wide-scale comparisons, and cannot be considered as reference basins.

Lastly, arguments in favor of the Brécý depocenter being part of a new wider-scale reference basin (which would be useful for further large-scale correlations, and located in between the two poles represented by the LOCPB of the southern Massif Central and Germany) include: its large preserved thickness (up to 3.9 kilometers), structural record (syn- and then post-rift stages) and age calibration (paleontological and absolute ages from deep wells and comparison with close connected basins with absolute temporal calibrations).

## 6. Summary and conclusion

The structural pattern, thickness, tectonic evolution and depositional environments of the late Carboniferous–Permian Brécý depocenter are revealed based on the reprocessing and interpretation of 115 km of vintage seismic lines combined with deep well data.

The present-day geometry of the Brécý depocenter is controlled by seven major and eleven minor eastward dipping normal faults; all these faults were active during the Meso-Cenozoic period, and some of them were possibly connected to deep detachments active during the late Carboniferous–Permian

history. The maximum thickness of the Brécý depocenter is reevaluated and estimated to be 3900 m.

The filling indicates a thick late Carboniferous–early Permian syn-rift stage overlain by a thin early to middle post-rift stage, similar to the tectonic evolution of the northeastward basins in Lorraine and Germany. The facies generally characterize lake environments, with occurrences of fluvial, alluvial and delta fan deposits. They mainly display a retrogradational–progradational pattern during the syn-rift stage, and a retrogradational pattern during the post-rift stage. The Brécý area is therefore the thickest depocenter known in the northern Massif Central by far. We propose that it was part of a larger basin during the latest Carboniferous–early Permian times, with a roughly W–E trend spanning more than four hundred kilometers in length in the northern Massif Central region. Strictly speaking, all the other so-called outcropping basins (Aumance, Decize-La-Machine, etc.) should be considered as depocenters, as they belong to a wider scale basin.

Because of the above features, this “northern Massif Central Carboniferous–Permian Basin” may be seen as a reference LOCPB, comparable to the basins known in the southern Massif Central, eastern France and Germany. Lastly, our work emphasizes the need for a further multi-method approach to explore LOCPB, especially their subsurface occurrences, as it is crucial to have a full view of these basins that contain information that is inaccessible to their outcropping remnants. It definitely highlights that LOCPB were obviously much wider and thicker than previously expected, with potential effective impacts on the understanding of the late Variscan tectonic and climatic evolution in France and western Europe.

## Declaration of interests

The authors do not work for, advise, own shares in, or receive funds from any organization that could benefit from this article, and have declared no affiliations other than their research organizations.

## Acknowledgements

This publication was initiated within the framework of the ICDP Deepdust project and was supported by the BRGM’s Research Division. The authors gratefully acknowledge François Baudin, coordinator of

this special issue dedicated to Jean Dercourt, for his patience and perseverance. They thank the two anonymous reviewers for their constructive comments, which have greatly improved the manuscript. The authors also thank Sara Mullin for proofreading the English content.

## References

- Aretz, A., Bär, K., Götz, A. E., and Sass, I. (2016). Outcrop analogue study of Permocarboniferous geothermal sandstone reservoir formations (northern Upper Rhine Graben, Germany): impact of mineral content, depositional environment and diagenesis on petrophysical properties. *Int. J. Earth Sci.*, 105, 1431–1452.
- Arnold, J., Jacoby, W. R., Schmeling, H., and Schott, B. (2001). Continental collision and the dynamic and thermal evolution of the Variscan orogenic crustal root—numerical models. *J. Geodyn.*, 31, 273–291.
- Averbuch, O. and Piromallo, C. (2012). Is there a remnant Variscan subducted slab in the mantle beneath the Paris basin? Implications for the late Variscan lithospheric delamination process and the Paris basin formation. *Tectonophysics*, 558–559, 70–83.
- Baptiste, J., Martelet, G., Faure, M., Beccaletto, L., Reninger, P.-A., Perrin, J., and Chen, Y. (2016). Mapping of a buried basement combining aeromagnetic, gravity and petrophysical data: The substratum of southwest Paris Basin, France. *Tectonophysics*, 683, 333–348.
- Barbarand, J., Quesnel, F., and Pagel, M. (2013). Lower Paleogene denudation of Upper Cretaceous cover of the Morvan massif and southeastern Paris basin (France) revealed by AFT thermochronology and constrained by stratigraphy and paléosurfaces. *Tectonophysics*, 608, 1310–1327.
- Barnolas, A. and Chiron, J.-C. (1996). *Synthèse géologique et géophysique des Pyrénées. Volume 1: Introduction. Géophysique. Cycle hercynien*. Edition BRGM, Orléans, ITGE, Madrid.
- Beccaletto, L., Capar, L., Serrano, O., and Marc, S. (2015). Structural evolution and sedimentary record of the Stephano-Permian basins occurring beneath the Mesozoic sedimentary cover in the southwestern Paris basin (France). *Bull. Soc. Géol. Fr.*, 186, 429–450.
- Beccaletto, L., Hanot, F., Serrano, O., and Marc, S. (2011). Overview of the subsurface structural pattern of the Paris Basin (France): Insights from the reprocessing and interpretation of regional seismic lines. *Mar. Pet. Geol.*, 28, 861–879.
- Bertrayl (1987). Rapport de fin de sondage. Esso Rep, 24 p.
- Blès, J.-L., Bonijoly, D., Castaing, C., and Gros, Y. (1989). Successive post-Variscan stress fields in the French Massif Central and its borders (western European plate); comparison with geodynamic data. *Tectonophysics*, 169, 79–111.
- Bois, C., Gabriel, O., and Pinet, B. (1991). Les campagnes sismiques SWAT et WAM, leur réalisation et leur interprétation par une équipe du programme ECORS. *Mém. Soc. Géol. Fr.*, 159, 9–24.
- Bonijoly, D. and Castaing, C. (1983). Fracturation et genèse des bassins stéphaniens du Massif central français en régime compressif. *Ann. Soc. Géol. Nord*, CIII, 187–199.
- Bouchot, V., Ledru, P., Lerouge, C., Lescuyer, J. L., and Milesi, J. P. (2005). Late Variscan mineralizing systems related to orogenic processes: The French Massif Central. *Ore Geol. Rev.*, 27(1–4), 169–197.
- Bouchot, V., Milesi, J.-P., Lescuyer, J.-L., and Ledru, P. (1997). Les minéralisations aurifères de la France dans leur cadre géologique autour de 300 Ma. *Chron. de la Rech. Minière*, 528, 13–62. (with map at 1/1,000,000).
- Bourquin, S., Guillocheau, F., and Péron, S. (2009). Braided river within an arid alluvial plain (example from the early Triassic, western German Basin): criteria of recognition and expression of stratigraphic cycles. *Sedimentology*, 56, 2235–2264.
- Bourquin, S., Peron, S., and Durand, M. (2006). Lower Triassic sequence stratigraphy of the western part of the Germanic basin (west of Black Forest): fluvial system evolution through time and space. *Sediment. Geol.*, 186, 187–211.
- Brécyl (1966). Rapport de fin de sondage. IDEHCO H 40, Compagnie d'exploration pétrolière, 15 p.
- Breitkreuz, C., Ehling, B.-C., and Sergeev, S. (2009). Chronological evolution of an intrusive/extrusive system: the Late Paleozoic Halle Volcanic Complex in the northeastern Saale Basin (Germany). *Z. Dtsch. Ges. Geowiss.*, 160(2), 173–190.
- BRGM (1970). *Notice de la carte géologique au 1/50000 de Saint-Etienne*. Edition BRGM, Orléans. feuille 745.

- BRGM (1976). *Notice de la carte géologique au 1/50000 de Montceau-les-Mines*. Edition BRGM, Orléans. feuille 578.
- BRGM (1984). *Synthèse géologique du Sud-Est de la France*, volume 126 of *Mém. du Bureau de Rech. Géol. Minières*. Edition BRGM, Orléans.
- BRGM (1989). *Synthèse géologique des bassins permien français*, volume 128 of *Mém. du Bureau de Rech. Géol. Minières*. Edition BRGM, Orléans.
- BRGM (2003). *Carte géologique de la France au 1/1000000ème*. 6ème édition révisée. Edition BRGM, Orléans.
- Bruguier, O., Becq-Giraudon, J. F., Champenois, M., Deloule, E., Ludden, J., and Mangin, D. (2003). Application of *in situ* zircon geochronology and accessory phase chemistry to constraining basin development during post-collisional extension: a case study from the French Massif Central. *Chem. Geol.*, 201, 319–336.
- Burg, J. P., Van Den Driessche, J., and Brun, J. P. (1994). Syn- to post-thickening extension: mode and consequences. *C. R. Acad. Sci. Ser. IIA*, 319(2), 1019–1032.
- Capuzzo, N., Handler, R., Neubauer, F., and Wetzel, A. (2003). Post-collisional rapid exhumation and erosion during continental sedimentation: the example of the late Variscan Salvain-Doré naz basin (Western Alps). *Int. J. Earth Sci.*, 92, 364–379.
- Cassinis, G., Perotti, C. R., and Ronchi, A. (2012). Permian continental basins in the Southern Alps (Italy) and peri-mediterranean correlations. *Int. J. Earth Sci.*, 101, 129–157.
- Chantraine, J., Lorenz, C., Mégnien, C., Million, R., and Lienhardt, M.-J. (1992). Forage scientifique de Sancerre-Couy (Cher): Synthèse d'études 1986–1992. *Mém. du Bureau de Rech. Géol. Minières, Géol. Profonde de la Fr.*, 3, 1–230.
- Chen, Y., Henry, B., Faure, M., Becq-Giraudon, J. F., Talbot, J. Y., Daly, L., and Goff, M. L. (2006). New Early Permian paleomagnetic results from the Brive basin (French Massif Central) and their implications for Late Variscan tectonics. *Int. J. Earth Sci.*, 95, 306–317.
- Choulet, F., Faure, M., Fabbri, O., and Monié, P. (2012). Relationships between magmatism and extension along the Autun-La Serre fault system in the Variscan Belt of the eastern French Massif Central. *Int. J. Earth Sci. (Geol. Rundsch)*, 101, 393–413.
- Costa, S. and Maluski, H. (1988). Datations par la méthode  $^{39}\text{Ar}$ - $^{40}\text{Ar}$  de matériel magmatique et métamorphique paléozoïque provenant du forage de Couy-Sancerre (Cher, France). Programme G.P.F. *C. R. Acad. Sci. Paris*, 306(II), 351–356.
- Costa, S. and Rey, P. (1995). Lower crustal rejuvenation and growth during post-thickening collapse: Insights from a crustal cross section through a Variscan metamorphic core complex. *Geology*, 23(10), 905–908.
- Courel, L., Donsimoni, M., and Mercier, D. (1986). La place du charbon dans la dynamique des systèmes houillers intramontagneux. *Mém. Soc. Géol. Fr.*, 149, 37–50.
- Delmas, J., Houël, P., and Vially, R. (2002). Paris Basin, Petroleum potential. IFP regional report.
- Dill, H., Teschner, M., and Wehner, H. (1991). Geochemistry and lithofacies of Permo-Carboniferous rocks from the southwestern edge of the Bohemian massif (Germany). A contribution to facies analysis of continental anoxic environments. *Int. J. Coal Geol.*, 18, 251–291.
- Domeier, M. and Torsvik, T. H. (2014). Plate tectonics in the late Paleozoic. *Geosci. Front.*, 5, 303–350.
- Donsimoni, M. (1990). Le gisement de charbon de Lucenay-lès-Aix (Nièvre). Documents du BRGM 179.
- Ducassou, C., Mercuzot, M., Bourquin, S., Rossignol, C., Pellenard, P., Beccaletto, L., Poujol, M., Hallot, E., Pierson-Wickmann, A. C., Hue, C., and Ravier, E. (2019). Sedimentology and U-Pb dating of Carboniferous to Permian continental series of the northern Massif Central (France): Local palaeogeographic evolution and larger scale correlations. *Palaeogeogr. Palaeoclimatol. Palaeoecol.*, 533, article no. 109228.
- Durand, M. (2014). Le bassin permien de saint-Dié-Villé (lorraine- alsace) et sa couverture gréseuse triasique. *Bull. Inf. Géol. du Bassin Paris*, 51(3), 3–24.
- Echtler, H. and Malavieille, J. (1990). Extensional tectonics, basement uplift and Stephano-Permian collapse basin in a late Variscan metamorphic core complex (Montagne Noire, Southern Massif Central). *Tectonophysics*, 177, 125–138.
- Faure, M. (1995). Late orogenic carboniferous extensions in the Variscan French Massif Central. *Tectonics*, 14, 132–153.
- Fischer, J., Schneider, J. W., Voigt, S., Joachimski, M. M., Tichomirowa, M., Tütken, T., Götze, J., and



- Berner, U. (2013). Oxygen and strontium isotopes from fossil shark teeth: Environmental and ecological implications for Late Palaeozoic European basins. *Chem. Geol.*, 342, 44–62.
- Gand, G. (2003). Le bassin permien de Blanzly-Le Creusot et ses bordures carbonifères. *Bull. Inf. Géol. du Bassin Paris*, 40(3), 4–19.
- Gand, G., Garric, J., Schneider, J., Sciau, J., and Walter, H. (1996). Biocénoses à méduses du permien français (bassin de Saint-Affrique, Massif Central). *Geobios*, 29(4), 379–400.
- Gardien, V., Martelat, J.-E., Leloup, P.-H., Mahéo, G., Bevilard, B., Allemand, P., Monié, P., Paquette, J.-L., Grosjean, A.-S., Faure, M., Chelle-Michou, C., and Fellah, C. (2022). Fast exhumation rate during late orogenic extension: The new timing of the Pilat detachment fault (French Massif Central, Variscan belt). *Gondwana Res.*, 103, 260–275.
- Gast, R. E., Dusar, M., Breitreuz, C., Gaupp, R., Schneider, J. W., Stemmerik, L., Geluk, M. C., Geisler, M., Kiersnowski, H., Glennie, K. W., Kabel, S., and Jones, N. S. (2010). Rotliegend. In Doornenbal, J. C. and Stevenson, A. G., editors, *Petroleum Geological Atlas of the Southern Permian Basin Area*, pages 101–121. EAGE Publications b.v., Houten.
- Gastaldo, R. A., DiMichele, W., and Pfefferkorn, H. (1996). Out of the icehouse into the greenhouse: a late paleozoic analog for modern global vegetational change. *GSA Today*, 6(10), 1–7.
- Gélard, J.-P., Castaing, C., Bonijoly, D., and Grolier, J. (1986). Structure et dynamique de quelques houillers limniques du Massif central. *Mém. Soc. Géol. Fr. Nouvelle Série*, 149, 57–72.
- Genna, A. and Debriette, P. J. (1994). Structures en fleur dans le bassin houiller d'Alès. Implications structurales. *C. R. Acad. Sci. Sér. 2 Sci. de La Terre et Des Planètes*, 318(7), 977–984.
- Goloubinoff, C. (1979). *Le permo-houiller du nord du bassin de St Affrique (Aveyron)*. Thèse de 3ème cycle, Université Paris-Sud. 143 p.
- Guillocheau, F., Robin, C., Allemand, P., Bourquin, S., Brault, N., Dromart, G., Friedenberg, R., Garcia, J.-P., Gaulier, J.-M., Gaumet, F., Grosdoy, B., Hanot, F., Le Strat, P., Mettraux, M., Nalpas, T., Prijac, C., Rigoltet, C., Serrano, O., and Grandjean, G. (2000). Meso-Cenozoic geodynamic evolution of the Paris Basin: 3D stratigraphic constraints. *Geodinam. Acta*, 13, 189–245.
- Hauville, B., Laine, C., Pélissier, N., Boka Mene, M., Jacob, Th., and Coppo, N. (2021). Exploration d'hélium en France : avancées du projet Fonts-Bouillants dans la Nièvre et résultats apportés par de multiples acquisitions géophysiques et géochimiques. RST2021 Lyon.
- Hemelsdaël, R., Averbuch, O., Beccaletto, L., Izart, A., Marc, S., Capar, L., and Michels, R. (2023). A deformed wedge-top basin inverted during the collapse of the Variscan belt: The Permo-Carboniferous Lorraine Basin (NE France). *Tectonics*, 42, article no. e2022TC007668.
- Henk, A. (1993). Late orogenic Basin evolution in the Variscan internides: the Saar-Nahe Basin, south-west Germany. *Tectonophysics*, 223, 273–290.
- Hertle, M. and Littke, R. (2000). Coalification pattern and thermal modelling of the Permo-Carboniferous Saar Basin, SW-Germany. *Int. J. Coal Geol.*, 42, 273–296.
- Hübner, N., Körner, F., and Schneider, J. (2011). Tectonics, climate and facies of the Saint Affrique Basin and correlation with the Lodève Basin (Permian, Southern France). *Z. Dtsch. Ges. Geowiss.*, 162(2), 157–170.
- Jacob, Th., Coppo, N., Dubois, F., Wawrzyniak, P., Portal, A., Bitri, A., Gaudot, I., Beccaletto, L., Le Maire, P., Laine, Ch., Hauville, B., and Pellissier, N. (2021). Exploration géophysique au sein du PER “Fonts-Bouillants” : apport des méthodes gravimétriques, audiomagnétotelluriques et électromagnétiques à source contrôlée. RST2021 Lyon.
- Juncal, M. A., Bourquin, S., Beccaletto, L., and Diez, J. B. (2018). New sedimentological and palynological data from the Permian and Triassic series of the Sancerre-Couy core, Paris Basin, France. *Geobios*, 51, 517–535.
- Kneuper, G. (1976). Regional geologische folgerungen aus der bohrung saar-1. *Geol. Jahrb.*, 27, 417–428.
- Knight, J. A. and Álvarez-Vázquez, C. (2021). A summary of upper Pennsylvanian regional substages defined in NW Spain—the chronostratigraphic legacy of Robert H. Wagner. *News. Stratigr.*, 54(3), 275–300.
- Laurent, A., Averbuch, O., Beccaletto, L., Graveleau, F., Lacquement, F., Capar, L., and Marc, S. (2021). 3-D structure of the variscan thrust front in Northern France: new insights from seismic reflection profiles. *Tectonics*, 40(7), 1–33.

- Lloret, J., Ronchi, A., López-Gómez, J., Gretter, N., De la Horra, R., Barrenechea, J. F., and Arche, A. (2018). Syn-tectonic sedimentary evolution of the continental late Palaeozoic-early Mesozoic Erill Castell-Estac Basin and its significance in the development of the central Pyrenees Basin. *Sediment. Geol.*, 374, 134–157.
- Lorenz, C., Mégnien, C., Delavenna, M., Galbrun, B., Gallet, Y., and Giot, D. (1987). Premiers résultats du sondage implanté sur l'anomalie magnétique du bassin de Paris, au Sud de Sancerre (Cher). Programme géologie profonde de la France. *C. R. Acad. Sci. Sér. 2, Méc. Phys. Chim. Sci. de l'univers, Sci. de la Terre*, 305(12), 1099–1104.
- Luccisano, V., Pradel, A., Amiot, R., Gand, G., Steyer, J.-S., and Cuny, G. (2021). A new Triodus shark species (Xenacanthidae, Xenacanthiformes) from the lowermost Permian of France and its paleobiogeographic implications. *J. Vertebr. Paleontol.*, 41(2), article no. e1926470.
- Lütznér, H., Tichomirowa, M., Käßner, A., and Gaupp, R. (2020). Latest Carboniferous to early Permian volcano-stratigraphic evolution in Central Europe: U-Pb CA-ID-TIMS ages of volcanic rocks in the Thuringian Forest Basin (Germany). *Int. J. Earth Sci.*, 110, 377–398.
- Malavieille, J. (1993). Late Orogenic extension in mountain belts: Insights from the basin and range and the Late Paleozoic Variscan Belt. *Tectonics*, 12, 1115–1130.
- Malavieille, J., Guihot, P., Costa, S., Lardeaux, J. M., and Gardien, V. (1990). Collapse of the thickened Variscan crust in the French Massif Central: Mont Pilat extensional shear zone and St. Etienne Late Carboniferous basin. *Tectonophysics*, 177, 139–149.
- Masclé, A. (1990). Géologie pétrolière des bassins permien français; Comparaison avec les bassins permien du Nord de l'Europe. Petroleum geology of French Permian basins; comparison with the Permian basins of northern Europe; Potentiel économique des bassins permien français. Economic potential of French Permian basins. *Chron. Rech. Minière*, 499, 69–86.
- Mathis, V. and Brulhet, J. (1990). Les gisements uranifères du bassin permien de Bourbon-l'Archambault (nord du Massif central français). *Chron. Rech. Minière*, 499, 19–30.
- Mattauer, M. and Matte, P. (1998). Le bassin Stéphanien de St-Etienne ne résulte pas d'une extension tardi-hercynienne généralisée : c'est un bassin pull-apart en relation avec un décrochement dextre. *Geodinam. Acta*, 11(1), 23–31.
- McCann, T., Kiersnowski, H., Krainer, K., Vozarova, A., Peryt, T. M., Oplustil, S., Stollhofen, H., Schneider, J., Wetzel, A., Boulvain, F., Dusar, M., Torok, A., Haas, J., Tait, J., and Koerner, F. (2008a). Permian. In McCann, T., editor, *The Geology of Central Europe; Precambrian and Palaeozoic 1*, pages 531–597. Geological Society of London, London, UK.
- McCann, T., Pascal, C., Timmerman, M. J., Krzywiec, P., López-Gómez, J., Wetzel, L., Krawczyk, C. M., Rieke, H., and Lamarche, J. (2006). Post-Variscan (end Carboniferous-Early Permian) basin evolution in western and central Europe. *Geol. Soc. Lond. Mem.*, 32(1), 355–388.
- McCann, T., Skompski, S., Poty, E., Dusar, M., Vozarova, A., Schneider, J., Wetzel, A., Krainer, K., Kornpohl, K., Schaefer, A., Krings, M., Oplustil, S., and Tait, J. (2008b). Carboniferous. In McCann, T., editor, *The Geology of Central Europe; Precambrian and Palaeozoic 1*, pages 411–529. Geological Society of London, London, UK.
- Ménard, G. and Molnar, P. (1988). Collapse of a Hercynian Tibetan plateau into a late Palaeozoic European Basin and Range province. *Nature*, 334, 235–237.
- Mercuzot, M., Bourquin, S., Beccaletto, L., Ducassou, C., Rubi, R., and Pellenard, P. (2021). Palaeoenvironmental reconstitutions at the Carboniferous-Permian transition south of the Paris Basin, France: implications on the stratigraphic evolution and basin geometry. *Int. J. Earth Sci. (Geol. Rundsch)*, 110, 9–33.
- Mercuzot, M., Bourquin, S., Pellenard, P., Beccaletto, L., Schnyder, J., Baudin, F., Ducassou, C., Garel, S., and Gand, G. (2022). Reconsidering Carboniferous-Permian continental paleoenvironments in eastern equatorial Pangea: facies and sequence stratigraphy investigations in the Autun Basin (France). *Int. J. Earth Sci.*, 111, 1663–1696.
- Mercuzot, M., Rossignol, C., Bourquin, S., Ramezani, J., Ducassou, C., Poujol, M., Beccaletto, L., and Pellenard, P. (2023). U-Pb age constraints on the Carboniferous-Permian transition in continental basins of eastern equatorial Pangaea (France): implications for the depositional history and correlations across the late Variscan Belt. *J. Geol. Soc.*, 180(6), article no. jgs2023-075.

- Michel, L. A., Tabor, N. J., Montañez, I. P., Schmitz, M. D., and Davydov, V. I. (2015). Chronostratigraphy and paleoclimatology of the Lodève Basin, France : evidence for a pan-tropical aridification event across the Carboniferous-Permian boundary. *Palaeogeogr. Palaeoclimatol. Palaeoecol.*, 430, 118–131.
- Montañez, I. P., Tabor, N. J., Niemeier, D., DiMichele, W. A., Frank, T. D., Fielding, C. R., Isbell, J. L., Birgenheier, L. P., and Rygel, M. C. (2007). CO<sub>2</sub>-forced climate and vegetation instability during Late Paleozoic deglaciation. *Science*, 315(5808), 87–91.
- Neumann, E.-R., Wilson, M., Heeremans, M., Spencer, E. A., Obst, K., Timmerman, M. J., and Kirstein, L. (2004). Carboniferous-Permian rifting and magmatism in southern Scandinavia, the North Sea and northern Germany: a review. In *Permo-Carboniferous Magmatism and Rifting in Europe*, Geological Society, London, Special Publications, 223, pages 11–40. Geological Society of London.
- Olivier, M., Bourquin, S., Desaubliaux, G., Ducassou, C., Rossignol, C., Daniau, G., and Chaney, D. (2023). The Late Paleozoic Ice Age in western equatorial Pangea: Context for complex interactions among aeolian, alluvial, and shoreface sedimentary environments during the Late Pennsylvanian early Permian. *Gondwana Res.*, 124, 305–338.
- Opluštil, S., Schmitz, M., Cleal, C. J., and Martínek, K. (2016). A review of the Middle-Late Pennsylvanian west European regional substages and \_oral biozones, and their correlation to the Geological Time Scale based on new U-Pb ages. *Earth Sci. Rev.*, 154, 301–335.
- Orszag-Sperber, F., Freytet, P., and Lebreton, M. L. (1992). Le Permien du forage de Sancerre-Couy: depots de plaine d'inondation. *Géol. Fr.*, 3–4, 43–49.
- Paquette, Y. (1980). *Le Bassin autunien de l'Aumance (Allier): sédimentologie (charbon, cinérites...), tectonique syndiagénétique*. Thèse de doctorat. 278 p.
- Pellenard, P., Gand, G., Schmitz, M., Galtier, J., Broutin, J., and Stéyer, J.-S. (2017). High-precision U-Pb zircon ages for explosive volcanism calibrating the NW European continental Autunian stratotype. *Gondwana Res.*, 51, 118–136.
- Pharaoh, T. C., Duser, M., Geluk, M. C., Kockel, F., Krawczyk, C. M., Krzywiec, P., Scheck-Wenderoth, M., Thybo, H., Vejbæk, O. V., and Van Wees, J. D. (2010). Tectonic evolution. In Doornenbal, J. C. and Stevenson, A. G., editors, *Petroleum Geological Atlas of the Southern Permian Basin Area*, pages 25–57. EAGE Publications b.v., Houten.
- Pittau, P., Barca, S., Cocherie, A., Del Rio, M., Fanning, M., and Rossi, P. (2002). Le bassin permien de Guardia Pisano (Sud-Ouest de la Sardaigne, Italie): palynostratigraphie, paléophytogéographie, corrélation et âge radiométrique des produits volcaniques associés. *Geobios*, 35(5), 561–580.
- Pochat, S. and Van Den Driessche, J. (2011). Filling sequence in Late Paleozoic continental basins: A chimera of climate change? A new light shed given by the Graissessac-Lodève basin (SE France). *Palaeogeogr. Palaeoclimatol. Palaeoecol.*, 302, 170–186.
- Poujol, M., Mercuzot, M., Lopez, M., Bourquin, S., Bruguier, O., Hallot, E., and Beccaletto, L. (2023). Insights on the Permian tuff beds from the Saint-Affrique Basin (Massif Central, France): an integrated geochemical and geochronological study. *C. R. Géosci.*, 355, 1–25.
- Prijac, C., Doin, M. P., Gaulier, J. M., and Guillocheau, F. (2000). Subsidence of the Paris Basin and its bearing on the late Variscan lithosphere evolution: a comparison between Plate and Chablis models. *Tectonophysics*, 323, 1–38.
- Retallack, G. J. (1988). Field recognition of paleosols. In Reinhardt, J. and Sigleo, W. R., editors, *Paleosols and Weathering Through Geologic Time: Principles and Applications*, Geological Society of America, Special Paper, 216, pages 1–20. Geological Society of America.
- Robin, C., Guillocheau, F., Allemand, P., Bourquin, S., Dromart, G., Gaulier, J.-M., and Prijac, C. (2000). Echelles de temps et d'espace du contrôle tectonique d'un bassin flexural intracratonique; le bassin de Paris. *Bull. Soc. Géol. Fr.*, 171, 181–196.
- Roig, J. Y., Alabouvette, B., Collomb, P., Bogdanoff, S., Guérangé-Lozes, J., Genna, A., Couturié, J. P., Monchoux, P., and Ciszak, R. (2001). *Notice explicative, Carte géol. France (1/50,000), feuille Decazeville (859)*. BRGM, Orléans. 94 p. Carte géologique par J. Y. Roig et al. (2001).
- Rolando, J.-P. (1988). *Sédimentologie et stratigraphie du bassin Permien de Saint-Affrique (Aveyron)*. Thèse de 3ème cycle, Université Paul Sabatier, Toulouse. 226 p.

- Schäfer, A. (2011). Tectonics and sedimentation in the continental strike-slip Saar-Nahe Basin (Carboniferous-Permian, West Germany). *Z. Dtsch. Ges. Geowiss.*, 162, 127–155.
- Schäfer, A. and Korsch, R. J. (1998). Formation and sediment fill of the Saar-Nahe basin (Permo-Carboniferous, Germany). *Z. Deutsch. Geol. Ges.*, 149(2), 233–269.
- Schneider, J. and Romer, R. L. (2010). The Late Variscan Molasses (Late Carboniferous to Late Permian) of the Saxo-Thuringian Zone. In Linnemann, U. and Romer, R. L., editors, *Pre-Mesozoic Geology of Saxo-Thuringia—From the Cadomian Active Margin to the Variscan Orogen*, pages 323–346. Schweizerbart, Stuttgart.
- Schneider, J. W., Körner, F., Roscher, M., and Kroner, U. (2006). Permian climate development in the northern peri-Tethys area—The Lodève basin, French Massif Central, compared in a European and global context. *Palaeogeogr. Palaeoclimatol. Palaeoecol.*, 240, 161–183.
- Schneider, J. W., Lucas, S. G., Scholze, F., Voigt, S., Marchetti, L., Klein, H., Opluštil, S., Werneburg, R., Golubev, V. K., Barrick, J. E., Nemyrovska, T., Ronchi, A., Day, M. O., Silantiev, V. V., Rößler, R., Saber, H., Linnemann, U., Zharinova, V., and Shen, S.-Z. (2020). Late Paleozoic-early Mesozoic continental biostratigraphy—Links to the Standard Global Chronostratigraphic Scale. *Palaeoworld*, 29, 186–238.
- Schneider, J. W. and Scholze, F. (2018). Late Pennsylvanian-Early Triassic conchostracan biostratigraphy: a preliminary approach. In *The Permian Timescale*, Geological Society, London, Special Publications, 450, pages 365–386. Geological Society of London.
- Scotese, C. R. and Langford, R. (1995). *Pangea and the paleogeography of the Permian, The Permian of northern Pangea; Volume I, Paleogeography, paleoclimates, stratigraphy*. Springer-Verlag, Germany.
- Serrano, O., Delmas, J., Hanot, F., Vially, R., Herbin, J. P., Houel, P., and Tourlière, B. (2006). Le bassin d'Aquitaine : Valorisation des données sismiques, cartographie structurale et potentiel pétrolier. Rapport Régional d'Evaluation Pétrolière, Ed. BRGM, 245 p.
- Soreghan, G. S., Beccaletto, L., Benison, K. C., Bourquin, S., Feulner, G., Hamamura, N., Hamilton, M., Heavens, N. G., Hinnov, L., Huttenlocker, A., Looy, C., Pfeifer, L. S., Pochat, S., Sardar Abadi, M., Zambito, J., and the Deep Dust workshop participants (2020). Report on ICDP Deep Dust workshops: probing continental climate of the late Paleozoic icehouse-greenhouse transition and beyond. *Sci. Drill.*, 28, 93–112.
- St. Georges-sur-Moulon1 (1964). Rapport de fin de sondage, EMESCO 250, Compagnie d'exploration pétrolière. 20 p.
- Stampfli, G. M., Hochard, C., Vérard, C., Wilhem, C., and vonRaumer, J. (2013). The formation of Pangea. *Tectonophysics*, 593, 1–19.
- Stille, H. (1924). *Grundfragen vergleichender Tektonik*. Borntraeger, Berlin.
- Stollhofen, H. (1998). Facies architecture variations and seismogenic structures in the Carboniferous-Permian Saar-Nahe Basin (SW Germany): evidence for extension-related transfer fault activity. *Sediment. Geol.*, 119, 47–83.
- Tabor, N. J. and Montañez, I. P. (2004). Morphology and distribution of fossil soils in the Permian-Pennsylvanian Wichita and Bowie Groups, north-central Texas, USA: implications for western equatorial Pangean palaeoclimate during icehouse-greenhouse transition. *Sedimentology*, 51(4), 851–884.
- Timmerman, M. J. (2004). Timing, geodynamic setting and character of Permo-Carboniferous magmatism in the foreland of the Variscan Orogen, NW Europe. In *Permo-Carboniferous Magmatism and Rifting in Europe*, Geological Society, London, Special Publications, 223, pages 41–74. Geological Society of London.
- Toutin, N. (1980). *Le Permien continental de la Provence orientale (France)*. Thèse de doctorat. vol. 2, 594 p.
- Van Den Driessche, J. and Brun, J. P. (1989). Un modèle cinématique de l'extension paléozoïque supérieur dans le Sud du Massif Central. *C. R. Acad. Sci. Sér. 2 Mécanique, Physique, Chimie, Sciences de l'univers, Sciences de la Terre*, 309, 1607–1613.
- Van Den Driessche, J. and Brun, J. P. (1992). Tectonic evolution of the Montagne Noire (French Massif Central): a model of extensional gneiss dome. *Geodynam. Acta*, 5, 85–97.
- Vanderhaeghe, O., Laurent, O., Gardien, V., Moyen, J.-F., Gébelin, A., Chelle-Michou, C., Couzinié, S., Villaros, A., and Bellanger, M. (2020). Flow of partially molten crust controlling construction, growth and

- collapse of the Variscan orogenic belt: the geologic record of the French Massif Central. *Bull. Soc. Géol. Fr. Earth Sci. Bull.*, 191, article no. 25.
- Voigt, S., Schindler, T., Tichomirowa, M., Käßner, A., Schneider, J. W., and Linnemann, U. (2022). First high-precision U-Pb age from the Pennsylvanian-Permian of the continental Saar-Nahe Basin, SW Germany. *Int. J. Earth Sci. (Geol. Rundsch)*, 111, 2129–2147.
- Ziegler, P. A. (1990). *Geological Atlas of Western and Central Europe*. Shell Internationale Petroleum Maatschappij B.V. Geological Society Publishing House (Bath), The Hague, Netherlands.